

**STUDIES ON EROSION WEAR BEHAVIOUR OF ALUMINIUM-
3MAGNESIUM-10SILICON CARBIDE COMPOSITE**

A thesis submitted in partial fulfilment of the requirements for the degree of

Bachelor of technology

In

Metallurgical and Materials Engineering

By

Pratyasha Mohapatra (109MM0011)

Swayam Prakash Sahoo (109MM0488)



Department of Metallurgical and Materials Engineering
National Institute of Technology
Rourkela

2013

**STUDIES ON EROSION WEAR BEHAVIOUR OF ALUMINIUM-
3MAGNESIUM-10SILICON CARBIDE COMPOSITE**

A thesis submitted in partial fulfilment of the requirements for the degree of

Bachelor of technology

In
Metallurgical and Materials Engineering

By

Pratyasha Mohapatra (109MM0011)

Swayam Prakash Sahoo (109MM0488)

Under the guidance of

Dr.Subash Chandra Mishra



Department of Metallurgical and Materials Engineering
National Institute of Technology

Rourkela

2013



NATIONAL INSTITUTE OF TECHNOLOGY ROURKELA

CERTIFICATE

This is to certify that the thesis entitled “**Studies on Erosion Wear Behaviour of Al-3Mg-10SiC Composite**” submitted by Pratyasha Mohapatra (109MM0011) and Swayam Prakash Sahoo (109MM0488) in partial fulfilment of the requirements for the award of BACHELOR OF TECHNOLOGY Degree in Metallurgical and Materials Engineering at the National Institute of Technology, Rourkela (Deemed University) is an authentic work carried out by him under my supervision and guidance.

To the best of my knowledge, the matter embodied in the thesis has not been submitted to any other University/ Institute for the award of any degree or diploma.

Date:

Prof. Dr. S.C. Mishra

Department of Metallurgical and Materials
Engineering

National Institute of Technology Rourkela,

ACKNOWLEDGEMENT

It is an immense pleasure to express our deep sense of gratitude to **Prof. Subash Chandra Mishra** our guide and supervisor for his invaluable guidance, motivation and constant inspiration. We also express our sincere thanks to the Department of Metallurgical and Materials Engineering for all the help and coordination extended by the department.

We are extremely thankful to **Prof. B.C. Ray**, Head of the Department, Metallurgical and Materials Engineering, **Prof A.Mallik** for their valuable help and advice during the course of this work.

We are also grateful to **Prof S.K. Acharya**, Department of Mechanical Engineering for his valuable time and cooperation for the completion of this work.

We are greatly thankful to the staff members of the department, all our well wishers, classmates and friends for their inspiration and help.

Date:

Pratyasha Mohapatra

Place:

Roll No: 109MM0011

Swayam Prakash Sahoo

Roll no: 109MM0488

Department of Metallurgical and Materials Engineering,
National Institute Of Technology, Rourkela
Rourkela-769008

ABSTRACT

Aluminum based metal matrix composites (MMCs) offer potential for advanced structural applications when high specific strength and modulus, as well as good elevated temperature resistance along with light weight, are important. In the present work, aluminum alloy-silicon carbide composite Al-3Mg-10SiC, developed using a stir casting technique is studied for wear behavior. Aluminium matrix composites finds its application in various fields like automobiles, aircraft, space equipment, structural components etc. Tribological characterization of aluminium matrix composites is critical for increasing its life and performance, particularly in fields of automobiles, aerospace and tooling, where failures from friction and wear can be catastrophic. Wear and friction manifest ultimately in loss of money in the form of energy loss and material loss. It leads to decrease in national productivity. Reduction in wear losses thus becomes essential for quality life. Thus tribology knowledge is important and significant for capital saving and hence this particular composite has been studied for tribological properties.

Solid particle erosion on Al-3Mg-10SiC was conducted under various parameters. Microstructural characterization of the surfaces and cross sections, micro-hardness measurement, X - ray diffraction studies were also studied. Implementation of design of experiments through Taguchi and statistical techniques in analyzing the erosion behavior of composites is discussed. The dependence of the wear rate on the parameters is studied and the wear mechanism is investigated by electron microscopy.

Variation of cumulative mass loss for different impingement angles were plotted and analysed. Initial mass loss is high, then it becomes sluggish and again after sometime there is sharp increase in mass loss. This increase is attributed to development of porous regions on the surface and tearing of grains on the surface.

Individual effects of control parameters are also analysed. It was clear from the Taguchi analysis that, of all the parameters affecting the wear rate, "velocity" is the most significant parameter while parameter "angle" also has some significant effect. Surface roughness is also measured.

It is evident that the predicted ANN results show a good agreement with the experimental sets. The optimized ANN structure further permits to study the effect of each of the control input parameters.

The hardness and tensile strength were also measured.

CONTENTS

1. INTRODUCTION	1
1.1 Research Background	2
1.2 Objectives of Research	5
2. LITERATURE SURVEY	6
2.1 Aluminium alloys	7
2.1.1 Properties of Aluminium alloys	7
2.1.2 Uses of Aluminum and their alloys	7
2.1.3 Aluminium-Magnesium alloys	9
2.2 Aluminium Metal Matrix Composite (AMC)	10
2.2.1 Advantages of AMC	10
2.2.2 Types of AMCs	11
2.3 Tribology	11
2.4 Wear	13
2.5 Types of Wear	14
2.5.1 Abrasive Wear	14
2.5.2 Adhesive Wear	15
2.5.3 Surface Fatigue Wear	15
2.5.4 Corrosive Wear	16

2.5.5 Erosion Wear	16
2.6 Mechanism of Solid particle erosion wear	17
2.7 Introduction To Statistical Techniques	23
2.7.1 Taguchi Method	23
2.7.2 ANN Analysis	24
3. EXPERIMENTAL DETAILS	28
3.1 Introduction	29
3.2 Sample Preparation	29
3.3 Erosion Wear	30
3.3.1 Design of Experiment	30
3.3.2 Test Apparatus	31
3.3.3 Experimental Procedure	33
3.4 Hardness Measurement	34
3.5 Roughness Measurement	34
4. RESULTS AND DISCUSSIONS	35
4.1 Taguchi Analysis	36
4.2 ANN Prediction of Erosion Wear Rate	38
4.3 Optical Microscopy	39
4.4 Phase Analysis	40

4.5 Hardness	40
4.6 Tensile Properties	41
4.7 Erosion Wear Test	41
4.7.1 Variation of Cumulative Mass Loss with Time	42
4.7.2 Effect of Angle of Impingement	44
4.7.3 Effect of Impingement Velocity	46
4.7.4 Effect of Stand-off Distance	47
4.8 Scanning Electron Microscopy	48
4.8.1 Fractured Surface of the Sample	48
4.8.2 Change in Surface Morphology with Erosion Time	48
4.9 Variation of Surface Roughness with Erosion Time	53
5. CONCLUSION	56
6. REFERENCES	58

LIST OF FIGURES

- Fig 2.1** Solid particle erosion wears. Erodent particles entrained in the fluid medium impact the target surface to cause material loss.
- Fig 2.2** The three layer neural network.
- Fig 3.1** Erosion wear test setup.
- Fig 3. 2** Schematic diagram of erosion test rig.
- Fig 4.1** Relative Effect of process parameters on erosion wear.
- Fig 4.3** Optical microstructures of Al-3Mg-10SiC cast metal matrix composite.
- Fig 4.4** XRD plot of the Al-3wt%Mg-10wt%SiC composite.
- Fig 4.7.1a** Variation of Cumulative Mass loss with time at 90° angle of impact, with a standoff distance of 20mm and impingement velocity of 60 m/s.
- Fig 4.7.1b** Variation of Cumulative Mass loss with time at 45° angle of impact, with a standoff distance of 10mm and impingement velocity of 45 m/s.

Fig 4.7.2 Variation of erosion rate on impingement angle for different impingement velocities of 15, 45, 60 and 75m/s at standoff distance fixed at 10mm.

Fig 4.7.3 Variation of erosion rate with impingement velocity for different impingement angles of 30°, 45°, 60° and 90° at standoff distance fixed at 10mm.

Fig 4.7.4 Variation of erosion rate with Standoff distance (SOD) for different impingement angles 60° and 90° at impingement velocity fixed at 60m/s.

Fig 4.8.1 Fractured surface of Al-3Mg-10SiC composite.

Fig 4.8.2.1a SEM micrograph of eroded sample at 90° after 2mins.
SOD : 20mm, Velocity of impingement: 60 m/s.

Fig 4.8.2.1b SEM micrograph of eroded sample at 90° after 4mins.
SOD : 20mm, Velocity of impingement: 60 m/s.

Fig 4.8.2.1c SEM micrograph of eroded sample at 90° after 6mins.
SOD : 20mm, Velocity of impingement: 60 m/s.

Fig 4.8.2.1d SEM micrograph of eroded sample at 90° after 8mins.
SOD : 20mm, Velocity of impingement: 60 m/s.

Fig 4.8.2.1e SEM micrograph of eroded sample at 90° after 10mins.
SOD : 20mm, Velocity of impingement: 60 m/s.

- Fig 4.8.2.2a** SEM micrograph of eroded sample at 45° after 10mins.
SOD : 10mm, Velocity of impingement: 45 m/s.
- Fig 4.8.2.2b** SEM micrograph of eroded sample at 45° after 10mins.
SOD : 10mm, Velocity of impingement: 45 m/s.
- Fig 4.8.2.2c** SEM micrograph of eroded sample at 45° after 10mins.
SOD : 10mm, Velocity of impingement: 45 m/s.
- Fig 4.8.2.2d** SEM micrograph of eroded sample at 45° after 10mins.
SOD : 10mm, Velocity of impingement: 45 m/s.
- Fig 4.8.2.2e** SEM micrograph of eroded sample at 45° after 10mins.
SOD : 10mm, Velocity of impingement: 45 m/s.
- Fig 4.9.1** Variation of the surface roughness of the Al-3Mg-10SiC composite during the erosion time of 10mins. Angle of impact: 90° SOD : 20mm, Velocity of impingement: 60 m/s.
- Fig 4.9.2** Variation of the surface roughness of the Al-3Mg-10SiC composite during the erosion time of 10mins. Angle of impact: 45° SOD : 10mm, Velocity of impingement: 45 m/s.

LIST OF TABLES

Table 1.	Input parameters selected for training
Table 2.	Erosion test parameters
Table 3.	Response Table for Means
Table 4	Experimental and ANN predicted values which are well in accordance
Table 5.	Tensile properties of the sample

Chapter 1

INTRODUCTION

- Objectives of the present piece of investigation
- Background

1.1 Research Background

Metal matrix composites have been developed and studied extensively in the past decade. The demand for metal matrix composites in the ever expanding fields of automobiles and aerospace industries and construction applications is increasing rapidly since the past three industrial revolutions. Metal matrix composites offer a variety of properties which are much superior to their monolithic counterparts. Metal matrix composites (MMCs) have been reported to have improved strength to weight ratio, higher specific modulus and better wear properties [1]. Among all the metal matrix composites in use, Aluminium metal matrix composites form a significant part. In recent past, Aluminium-base composites have potentially grown in engineering and structural applications starting from automobile & construction industries to marine and aerospace industries. Aluminium is one of the most versatile elements, available abundantly on the earth. Aluminium has a very unique combination of physical and mechanical properties which can be engineered to suit a wide variety of applications [1]. Aluminium is light weight, has high strength to weight ratio, good thermal and electrical conductivity and thermal coefficient of expansion. Addition of alloying elements like Magnesium, Copper and Silicon etc. is done in order to further improve the properties. These Aluminium and its alloys(like with Magnesium, Copper etc.) reinforced with ceramics, due to their exceptional combination of properties, have become one of the most suitable candidates for applications in ship and submarine building, transportation, heavy vehicles, pressure vessels, bridges, buildings, automobile and aircraft parts and braking systems.

The Aluminium-Magnesium-SiC MMC are very light weight, have high strength to weight ratio, high specific strength, high specific rigidity easily weld able and improved wear properties. The light weight of these alloys help in reducing the fuel consumption, thus enhancing the fuel efficiency [2]. Further, the strengthening of aluminium alloys with a

dispersion of fine ceramic particulates has dramatically increased their potential for wear resistant applications. Moreover as these metal matrix composites are extensively used in construction applications, they are subjected to different adverse conditions which result in wear and deterioration during service. Thus it becomes very vital to study the wear behaviour of these composites.

In the present work, the material being worked upon is Aluminium-3wt% Magnesium reinforced with 10 wt% SiC. Magnesium being lighter than aluminium further reduces the alloy density when added to aluminium and also improves the wettability, formability and strength by age hardening. But alloys with more than 3 wt% Mg are not recommended for elevated temperature applications due to high susceptibility to stress corrosion cracking. SiC is one of the most widely used ceramic reinforcements in Aluminium metal matrix composites. SiC have high corrosion resistance, high thermal conductivity, low thermal expansion coefficient, high hardness and good refractory properties [2]. Addition of SiC to aluminium improves its strength and other mechanical and thermal properties. This material is highly suitable for structural applications and in automobile disc brake systems. During their use, the material is generally subjected to unproductive and harmful friction and continued impact by wind and erosive particles which leads to wear, material loss and damage to the structures. Wear leads to unwanted material losses and plays a very critical role in determining the life and suitability of the material for a particular application.

Tribological studies concern with the study of wear, friction and lubrication of surfaces in motion relative to each other. Tribological characterization of aluminium matrix composites is critical for increasing its life and performance, particularly in fields of automobiles, aerospace and tooling, where failures from friction and wear can be catastrophic.

Wear and friction manifest ultimately in loss of money in the form of energy loss and material loss. It leads to decrease in national productivity. Reduction in wear losses thus becomes essential for quality life.

Thus tribology knowledge is important and significant for capital saving and hence this particular composite has been studied for tribological properties.

The aim of the present work is to investigate the erosion wear behaviour of Aluminium-3wt%Magnesium reinforced with 10wt% Silicon Carbide developed by stir casting method. Solid particle erosion on Al-3Mg-10SiC is conducted using sand particles. Implementation of statistical techniques (through Taguchi and statistical techniques) in analyzing the erosion behavior of composites is made. The dependence of the wear rate on the parameters is studied and the surface morphology is investigated by electron microscopy. The dominant wear mechanisms governing the wear behavior are then studied from the SEM micrographs.

1.2 Objectives of Research

The objectives of the present piece of investigation are as follows:

- a) To determine the solid particle erosion wear rate by calculating the cumulative mass loss of the Al-3Mg-10SiC composite.
- b) To study the dominant mechanism governing the wear behaviour.
- c) To investigate the effect of operating parameter viz. impact angle, pressure on wear rate in solid particle erosion testing.

Chapter2

LITERATURE SURVEY

- Aluminium alloys
- Aluminium metal matrix composites
 - Tribology
 - Wear
 - Types of wear
- Industrial Applications of Plasma Spraying
 - Wear
 - Types of wear
- Mechanism of Solid particle erosion wear
- Introduction To Statistical Techniques

2.1 Aluminium alloys:

The growing demand to reduce energy consumption, resource depletion, air pollution and race to economic growth has led to the exploitation of aluminium and its alloys.

2.1.1) Properties of Aluminium alloys[3]:

- 1 Aluminium alloys exhibit high strength to weight ratios.
- 2 Al-alloys cover a wide range of values of strength, ranging from 10 N mm⁻² for elastic limit of pure Al to 500 N mm⁻² for 7000 series alloys.
- 3 Aluminium alloys are sufficiently ductile to be used in structural applications.
- 4 These alloys do not lose strength at low temperatures, in fact Al-Mg alloys show increase in their at low temperatures.
- 5 They are corrosion- resistant and possess good weld ability.
- 6 They exhibit high tensile strength.
- 7 Many Al alloys developed provide strength, wear resistance and hardness at elevated temperatures.

2.1.2) Uses of Aluminum and their alloys:

- Automobile Industry:

Aluminum is an ideal candidate to replace heavier metals in cars owing to its characteristic properties like high strength stiffness to weight ratio, good formability, corrosion resistance and recycling properties.

It is used in power-train, chassis, body structure and air-conditioning. Wrought aluminum is gaining its purpose in heat shields, bumper reinforcements, air-bag housings, pneumatic systems and seat frames. The high strength to weight ratio is the prime reason for its use in automotive sector as it leads to less fuel consumption.

Studies show that 10% weight reduction equals 5.5% improvement in fuel economy [4].

Aluminium-Magnesium alloys are used in disc brakes, forged wheels which experience extreme loading conditions.

- Aircraft Industry:

Aluminum, alloys with different element and finds its application in high working temperature and also in low temperature region of highly loaded parts with high resistance to corrosion under stress.

- Space equipment:

High values of specific strength and its high rigidity provides high longitudinal stability which enables it to be used in tanks, inner tank and casing of rocket

- Structural Applications:

Light weight and corrosion resistance makes it an ideal choice for its use in structural applications. The extrusion fabrication process makes it possible to increase the geometrical property of the cross-section by designing a shape that simultaneously gives the minimum weight and the highest structural efficiency. It is easy to obtain stiffened shapes without using built-up sections, thus avoiding welding or bolting. Lightness makes it easy to have simpler erection, transport of fully fabricated components and reduction of load transmitted to foundations [5].

- Al-Mg alloys are used in electrical contact resistors.

- Aluminum also is used for packaging, in containers (beverage cans).

- Aluminum is also used in cryogen conditions in contact with liquid H₂O, H₂ and He.

2.1.3) Aluminium-Magnesium alloys

Aluminium has several series in its nomenclature based on elements it alloys with. For example, 3XXX for alloying with manganese, 5XXX for alloying with magnesium and 6XXX for alloying with magnesium and silicon.

Advantages of magnesium additions to aluminium

- 1) Magnesium has two thirds the weight of Aluminium, thus addition of Magnesium to Aluminium leads to decrease in the density of the alloy.
- 2) Magnesium has higher specific strength than Aluminium. Thus addition of magnesium results in increased strength of alloy as compared to Aluminium.
- 3) Magnesium addition leads to an increase in the strength to weight ratio. Thus the alloys are more suitable for automobile and aircraft parts as it increases the fuel efficiency.
- 4) Addition of magnesium to aluminium results in precipitation and age hardening of alloy. Thus the strength is significantly
- 5) The most important advantage of Magnesium addition is that it improves the wettability of solid ceramic reinforcement in Aluminium metal matrix composites. Better wettability would result in more homogeneous distribution of reinforcement in the matrix.
- 6) Magnesium also improves the formability and castability of aluminium.

Problems associated with magnesium addition to aluminium during manufacturing by vortex method.

Addition of Magnesium to Aluminium is highly beneficial for different reasons as stated above. But addition of Magnesium to Aluminium during alloying is difficult.

The problems associated with the Magnesium addition are:

- 1) Magnesium is highly volatile, it has lower boiling point (1090°). Magnesium has lower density than Aluminium.
- 2) Magnesium being volatile, losses of magnesium during manufacturing by liquid route is very high.
- 3) Magnesium is highly reactive. Thus there are chances of violent uncontrolled explosive reactions during manufacturing process.

2.2 Aluminium Metal Matrix Composite (AMC):

Aluminium matrix composites (AMCs) refer to the class of light weight high performance aluminium centric material systems. The reinforcement in AMCs could be in the form of continuous/discontinuous fibres, whisker or particulates, in volume fractions ranging from a few percent to 70%. Properties of AMCs can be tailored to the demands of different industrial applications by suitable combinations of matrix, reinforcement and processing route [6].

2.2.1) Advantages of AMC

- 1) Greater strength
- 2) Improved stiffness
- 3) Reduced density(weight)
- 4) Improved high temperature properties
- 5) Controlled thermal expansion coefficient
- 6) Thermal/heat management
- 7) Enhanced and tailored electrical performance
- 8) Improved abrasion and wear resistance

- 9) Control of mass (especially in reciprocating applications)
- 10) Improved damping capabilities.

2.2.2) Types of AMCs

AMCs can be classified into four types depending on the type of reinforcement:

- (a) Particle-reinforced AMCs (PAMCs)
- (b) Whisker-or short fibre-reinforced AMCs (SFAMCs)
- (c) Continuous fibre-reinforced AMCs (CFAMCs)
- (d) Mono filament-reinforced AMCs (MFAMCs)

Some of the salient features of these four types of AMCs are detailed below.

Particle reinforced aluminium matrix composites (PAMCs)

These composites generally contain equi-axed ceramic reinforcements with an aspect ratio less than about 5. Ceramic reinforcements are generally oxides or carbides or borides (Al_2O_3 or SiC or TiB_2) and present in volume fraction less than 30% when used for structural and wear resistance applications. The material under study is Al-3wt%Mg-10wt%SiC. Addition of Silicon Carbide particles in AMCs improves the corrosion resistance, increases the thermal conductivity, strength, and refractory properties.

2.3 Tribology

Tribology is derived from a Greek word “tribos” means rubbing. It is the science and technology of interacting surfaces in relative motion and the practices related thereto; their design, friction, wear and lubrication [7].

In order to characterize the significance of tribology among other things, a few points have been emphasized [8]:

1.The economic aspect of tribology:

It has been estimated that about 30% of the energy generated in the industrial parts of the world is consumed ultimately in friction processes or that in highly industrialized countries like England, Japan or the republic of Germany, some \$2,000 million per annum are lost as a result of wear processes. Even if these figures are taken as rough estimates, they clearly indicate the importance of tribology for conservation of energy and materials. Tribological characterization is, therefore, critical for increasing material life and performance. Particularly in fields of aerospace, automotive and tooling, where failures from friction and wear can be catastrophic. Tribology is important in modern machinery in which sliding and rolling between surfaces occur. In automobiles, brakes, clutches, bolts, nuts, tires etc. use friction. In this case it is a productive friction. Unproductive friction and wear takes place in auto parts like engines, cams, gears, bearings etc. Friction and wear cost money in the form of energy loss and material loss. It leads to decrease in national productivity. Reduction in wear and friction can lead to quality of life. Thus tribology knowledge is important and significant for capital saving [8].

2.The scientific aspect of tribology:

It is well-known that all the macroscopic processes in nature are irreversible. Science in its pure theories has largely omitted this irreversibility since the laws of “ideal” processes were much easier to develop. Tribology should attempt to investigate the irreversible processes of mechanics in detail and to explain the complex effects of energy and material dissipation.

3.The multi-disciplinary aspect of tribology:

- Compatible coefficient of friction's requirement. If a natural lubricant from knee-joints is lost and has to be replaced/re-filled by artificial lubricant, tribological studies can help in calculating [8].
- It is through tribology know-how that makers of hard-disk drivers have been able to squeeze in more data in less and less space [8].

2.4 Wear

Wear is the damage incurred by a material surface due to the relative motion with other contacting surfaces which generally results in unproductive material losses. Wear can result in removal of material from either or both the contacting surfaces.

Wear is defined as “the damage to a solid surface, generally involving the progressive loss of material, due to relative motion between two moving surfaces [9]”.

But for engineering aspects wear can be defined in the following ways:

- 1) Wear is a damage to the material surface which results in “loss of material” from the surfaces. Apart from material lossess. Wear has other aspects to it.
- 2) As wear refers to the damage to the contacting surfaces, wear can be refered to “the movement of material” on the surface even if it doesnot involve material loss from the surface.
- 3) A third aspect of wear which includes the damage to the surface but not material loss or dimensional changes. A manifestation of this mode of wear may be by the formation of numerous networks of cracks on the surface. This mode becomes significant with optically transparent materials.

Thus wear is the damage to the material surface which adversely affects the life and performance of the part.

2.5 Types Of Wear

Wear can be classified into different types depending on whether it occurs in dry or lubricated conditions or types of wearing contacts.

Dry friction, which is the primary concern in the absence of lubricants or dry condition, is defined as friction under not intentionally lubricated conditions. But it is well known that it is friction under lubrication by atmospheric gases, especially by oxygen [10].

On the basis of type of wearing contacts, wear is either (i) Single-phase wear where one solid causes material removal from the sliding surface against which it is in relative motion.

(ii) Multi-phase wear, where wear, from a solid, liquid or gas acts as a carrier for a second phase that actually produces the wear.

A fundamental scheme for classifying wear was first outlined by Burwell and Strang [11].

Later Burwell [12] modified the classification to include five distinct types of wear, namely

- (1) Abrasive
- (2) Adhesive
- (3) Erosive
- (4) Surface fatigue
- (5) Corrosive

2.5.1 ABRASIVE WEAR

Most machine parts and sliding surfaces generally experience abrasive wear. Abrasive wear occurs when a hard surface slides or rubs against a softer surface. According to ASTM, abrasive wear occurs due to the hard particles or protuberances that are forced to move along the softer surface.

. Hard particles or asperities on the harder surface cut or groove the softer surface resulting in abrasive wear. The hard particles can be present on one of the sliding surfaces or may have originated from either of them. In sliding wear, the asperities on the harder surface produce the wear. Sometimes wear fragments torn from the surfaces get repeatedly plastically deformed and work hardened and even oxidized and become harder than either of the contacting surfaces, thus resulting in abrasive wear of both the surfaces. Abrasive particles may also be introduced from outside like dirt from outside the system.

There are different mechanisms of wear which operate during the abrasive wear, resulting in removal of material. These mechanisms are:

(a) Fatigue (b) fracture and (c) melting. The process of abrasion is complex and thus is a combination of all the mechanisms operating simultaneously. The abrasion process includes ploughing, cutting, wedge formation, microfatigue and microcracking.

2.5.2 ADHESIVE WEAR

Adhesive wear occurs when two surfaces are in very close contact with each other. In adhesive wear, a localised bonding occurs between the solid surfaces in contact, which results in transfer of material from one surface to another or loss of material from both the surfaces. But this wear requires a very close contact between the interacting solid surfaces. Adhesive wear results in formation of seizures, rough and torn surfaces.

2.5.3 SURFACE FATIGUE WEAR

Fatigue is the failure caused by dynamic loading. Repeated loading can result in wear too. Thus the surface wear which is due to fracture arising from material fatigue is defined as surface fatigue wear. A network of microcracks is formed below the material surface due to the dynamic loading. When these cracks are subjected to cycles of repeated loading and

unloading, they propagate. After reaching the critical size, these subsurface microcracks grow rapidly and emerge at the surface, thus resulting in removal of flat sheets of detached particles. The appearance of the worn out surface includes sharp and angular edges around the pits formed.

2.5.4 CORROSSIVE WEAR

Corrosion is the degradation of a material due to some physiochemical reactions with the surrounding atmosphere. Corrosive wear may be defined as the gradual deterioration of an unprotected metal surface due to interactions with the surrounding media, like alkalis, acids and gases. Thin films are formed on the material surface due to different tribochemical reactions. Metals generally react with oxygen to form oxides. These oxides form a layer over the metal and may cause formation of layers of scales on the surface, as the interfacial bond is low with the underlying metal or alloy. The surface consists of rough pits, depressions, perforations. Corrosive wear is dangerous as it may result in complete dissolution of the metal.

2.5.5 EROSION WEAR

Erosive wear can be defined as metal removal due to impingement of solid particles on the material surface. The solid particles which impact the surface are at some velocity and thus possess kinetic energy and momentum. On striking the surface the particles dissipate their energy and momentum to the material surface resulting in removal of material and formation of grooves. Erosion may be caused by solid particles or even by a gas or a liquid, which may or may not carry solid particles, impinging on a surface. The impact of the erodent causes the wear to occur. Erosion wear results in significant damage to structural materials in case of sand blasting or in pipelines carrying slurry and thus should be taken care of.

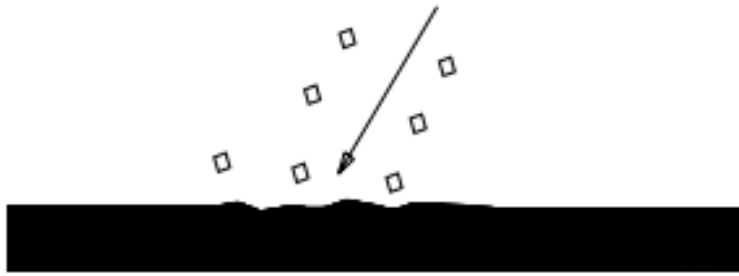


Fig 2.1 Solid particle erosion wear. Erodent particles entrained in the fluid medium impact the target surface to cause material loss.

2.6 Mechanism of Solid particle erosion wear

In erosion wear process, particles are generally entrained in a fluid which may be a gas or a liquid and impinge the material surface under a given velocity. As the particles impact the surface at a certain velocity they possess kinetic energy and momentum. Thus the load applied by the erodent particle on the material surface is due to the momentum and the kinetic energy. An equation used for describing the erosion wear can be derived by a simple model of particle impact on test surface.

The equation can be then further modified to measure the differences in the wear during different loading conditions.

The erosion wear rate is said to be dependent on certain factors which control the erosion wear process of the material surface.

These process parameters are:

- (1) Angle of impingement
- (2) Impingement velocity
- (3) Standoff distance
- (4) Nature of Erodent
- (5) Material properties

The angle at which a particle impacts the material surface is known as the angle of impingement. The angle of impingement is a very important parameter in erosion wear. In erosion wear, the angle at which the erodent particles impinge the surface influences the rate at which material eroded from the material surface. The effect of angle of impingement can be studied by considering the impact of a single particle with a surface. The angle determines the relative magnitude of the two velocity components of the impact, i.e. the component that is normal to the surface and the one that is parallel to the surface. The normal component determines the magnitude of the impact on the surface. It will show the length of time (t) for which the impact will occur. The product of t and the tangential velocity component determine the amount of sliding that takes place. The tangential velocity component also provides a shear loading to the surface. This shear loading occurs in addition to the normal load produced by the normal velocity. Thus as the angle changes, the magnitude of the two components change and thus the loading system also changes. The change in the loading system would result in the change in the mechanism causing wear.

The mechanism of wear is also dependant in the impinging angle. The mechanism of wear is different for different materials and generally includes cutting or machining in case of ductile materials and microcracking in case of brittle materials.

It has been demonstrated that the angle of impact i.e. the angle between leading edge of the particle and the material surface determine whether or not cutting occurs

Below a critical value, deformation takes place.

The normal component of the particle velocity (V_p) determines the contact time (t) and the load. The product of t and the tangential velocity component (V_t) determine the amount of sliding that takes place. The tangential component provides shear loading. In case of ductile materials, greater is the sliding, the material can accommodate the shear load by plastic deformation on the surface. Thus mechanisms like micromachining and micro cutting cause material erosion. The sliding component is greater at lower angles and thus ductile materials show maximum erosion at lower angles.

Brittle materials do not undergo plastic deformation. Rather normal impact of the particles results in generation of microcracks which eventually lead to material loss. Thus brittle materials show maximum erosion at 90° . For materials showing maximum erosion at intermediate angles, the cutting, ploughing and the microcracking mechanisms operate [36].

When the erosion wear occurs at normal angles of impingement, the weight of the material initially increases and then it attains a steady state called steady state erosion. The increase in weight of the material can be attributed to the initial embedment of particle in the target surface [36]. As the erosion wear occurs for longer durations of time, gradually these particles are removed from the surface and a steady state is attained [13-15]. At smaller angles of impingement the incubation period is less as, the normal component is smaller, associated with the erodent particles. The impact energy now is primarily utilised in sliding the particles and results in roughening the target surface [16].

The different processes involved with solid particle erosion are cutting, impact and fatigue processes. The local energy concentration of the erodent on the target surface is critical for the erosive wear [15, 17, 18].

Hitting of a particle corresponds to a certain impact force imposed on the material surface. During impact, the initial energy of the particle is converted into different energy terms [36].

The occurred impact is categorized in

- (a) Normal, elastic impact,
- (b) Normal, plastic impact,
- (c) Normal, elastic/plastic impact and
- (d) Oblique, elastic/plastic impact.

The work of different researchers working on erosion wear and Aluminum metal matrix composites have been studied and presented here.

A. Alahelisten, F. Bergman, M. Olsson and S. Hogmark[19] have studied the effect of fibre reinforcement in aluminium, magnesium and Mg-9Al-1Zn on the wear properties. It is observed that with the increase in the fibre content the erosion resistance of Aluminium and Magnesium decreases. This is due to the high tendency of the reinforced phase to cracking and fragmentation. It was observed that the direction of fibre alignment does not have a significant influence on the wear behaviour. The SEM micrographs of the abraded and the erode surfaces were identical.

The different wear mechanisms which operate during erosion have also been investigated and the dominant mechanism is found to be microcutting. As the content of reinforcing fibre is increased, the loss of material due to erosion is also enhanced due to excessive crack

formation at the fibre matrix interface and at the fibers. As Aluminium has higher ductility than Magnesium , it exhibits better erosion wear resistance and the dominant wear mechanism is microplooughing rather than microcutting.

J. D. Ayers [20] has studied the wear behavior of aluminum- and titanium-base alloys containing particles of TiC or WC introduced by the laser meltparticle injection process. Erosion wear experiments has been conducted on 6061 aluminum containing TiC. The erosion wear testing is done at very sever conditions and thus the impacting glass spheres which were used as erodents, deformed the metal matrix. The deformation was such that TiC particles well below the sample surface were fractured. These fractures initiated cracks inside the metal matrix. Thus due to the formation of cracks the erosion rate was enhanced and as a result the metal matrix alloy with carbide injected surface exhibited almost double the erosion than the base alloy. It was predicted again than under less severe conditions of erosion wear which would involve lower angles of impingement, the erosion wear resistance is predicted to be better.

TiC injected aluminum alloys are show poor erosion wear resistance when subjected to erosion by energetic particles at high impact angles.

R.Rattan,Jayashree Bijwe[21] have worked on the influence of the impingement angle on the solid particle erosion of carbon fibre reinforced polyetherimide composite. In their work the angle of impingement and the particle velocity were taken as the operating parameters. The study of the mode of erosion revealed that for ductile materials maximum erosion occurs at lower angles of erosion i.e. 15o to 30o while for brittle materials the same occurs at 90o. If the erosion is maximum within the range of 34o to 45o then mode of wear is considered to be semiductile. The study of mechanism of wear showed that ductile wear occurs with erosion

by formation and detachment of heavily strained surfaces where erodent contacts repeatedly. Material removal at lower angles occurs mainly by micromachining and cutting. When a particle strikes the surface, the two components of its velocity contribute to different wear mechanisms. The tangential component causes removal of material by lateral displacement while the normal component causes indentation. Thus for a ductile material, the impact at 90° results in deformation of the material backwards or forward in the plane of the surface, but the loss of material is insignificant. In brittle materials, the impact of the erodent particles result in formation of microcracks which link and grow to cause wear. In fibre reinforced composite materials, the fibres inhibit the growth of the microcracks in the matrix. The cracks propagate further by cracking the fibres.

S.wilson and A.Ball [22] have studied the wear resistance of 6000 series aluminium alloy, reinforced with silicon carbide particles through solid particle erosion, corrosion erosion, abrasion and sliding wear. The cavitation erosion of the MMCs are found to be similar to their monolithic alloy counterpart and the solid particle erosion resistance of the alloy is found to be better than the metal matrix composites

2.7 Introduction To Statistical Techniques

2.7.1 TAGUCHI METHOD

The Taguchi method is a powerful tool for designing high quality systems based on orthogonal array (OA) for designing the experiments with an optimum setting of process control parameters [23-27]. Because of this, each factor can be evaluated independently of all the other factors, so the effect of one factor does not influence the estimation of another factor. Taguchi method works on the effect of variation on the process quality characteristics rather than on its averages unlike the traditional experimental design procedures that emphasizes on the average process performance characteristics. That is, the Taguchi approach makes the process performance insensitive (robust) to variation in uncontrolled or noise factors. Here the simultaneous and independent analysis of two or more parameters for their ability to affect the variability of a particular product or process characteristic can be done in a minimum number of tests [28-30]. The Taguchi method surfs the entire design space through a small number of experiments in order to determine all of the parameter effects and several of the interactions. These data are then used to predict the optimum combination of the design parameters that will minimize the objective function and satisfy all the constraints. The parameter design phase of the Taguchi method generally includes the following steps: (1) identify the objective of the experiment; (2) identify the quality characteristic (performance measure) and its measurement systems; (3) identify the factors that may influence the quality characteristic, their levels and possible interactions; (4) select the appropriate OA and assign the factors at their levels to the OA; (5) conduct the test described by the trials in the OA; (6) analysis of the experimental data using the signal-to-

noise (S/N) ratio, factor effects. The (S/N) ratios are logarithmic functions of desired output which serve as objective functions for optimization. It takes both the mean and the variability into account and is defined as the ratio of the mean (signal) to the standard deviation (noise). The ratio depends on the quality characteristics of the product/process to be optimized. The three categories of S/N ratios are used: lower the better (LB), higher the better (HB) and nominal the best (NB). The parameter level combination that maximizes the appropriate S/N ratio is the optimal setting. This inexpensive and easy-to-operate experimental strategy based on Taguchi's parameter design has been adopted to study effect of various parameters and their interactions in a number of engineering processes.

2.7.2 ANN ANALYSIS

Erosion wear is considered as a non-linear problem with respect to its variables: either materials or operating conditions.. In order to control the erosion rate, one of the challenges nowadays is to recognize parameter interdependencies, correlations and individual effects on erosion characteristics. Therefore a robust methodology is needed to study these interrelated effects. A statistical method, responding to the previous constraints, is implemented to correlate the processing parameters to the erosion wear properties. This methodology is based on artificial neural networks (ANN), which is a technique that involves database training to predict property-parameter evolutions. This section presents the database construction, implementation protocol and a set of predicted results related to the erosion wear rate. ANNs are excellent tools for complex processes that have many variables and complex interactions. The analysis is made taking into account training and test procedure to predict the dependence of erosion wear behaviour on angle of impact and velocity of erodent. This technique helps in saving time and resources for experimental trials. The details of this methodology are described by Rajasekaran and Pai [33].

NEURAL NETWORK MODEL: Development and Implementation

An ANN [34] is a computational system that simulates the microstructure (neurons) of biological nervous system. The most basic components of ANN are modelled after the structure of brain. Inspired by these biological neurons, ANN is composed of simple elements operating in parallel. It is the simple clustering of the primitive artificial neurons. This clustering occurs by creating layers, which are then connected to one another. Some of the neurons interface the real world to receive input and other neurons provide the real world with the network's output. All the rest of the neurons are hidden from view. The multi-layered neural network being used extensively for material science research has been reviewed by Zhang and Friedrich [31]. A software package NEURALNET for neural computing developed by Rao and Rao [32] using back propagation algorithm. This software is presently being used for the prediction of erosion wear rate at different impact angles, velocities and stand-off distances.

Input Parameters for Training	Values
Error tolerance	0.003
Learning parameter(β)	0.002
Momentum parameter(α)	0.002
Noise factor (NF)	0.001
Maximum cycles for simulations	20,00,000
Slope parameter (ξ)	0.6
Number of hidden layer neuron	6
Number of input layer neuron (I)	3
Number of output layer neuron (O)	1

Table 1. Input parameters selected for training of ANN

The database is built considering experiments at the limit ranges of each parameter. Experimental result sets are used to train the ANN in order to understand the input-output correlations. The database is then divided into three categories, namely: a validation category, which is required to define the ANN architecture and adjust the number of neurons for each layer; a training category, which is exclusively used to adjust the network weights and a test category, which corresponds to the set that validates the results of the training protocol. The input variables are normalized so as to lie in the same range group of 0-1. To train the neural network used for this work, about 16 data sets on selected substrates are taken. It is ensured that these extensive data sets represent all possible input variations within the experimental domain. So a network that is trained with this data is expected to be capable of simulating the erosion wear rates. Different ANN structures (I-H-O) with varying number of neurons in the hidden layer are tested at constant cycles, learning rate, error tolerance, momentum parameter and noise factor and slope parameter. Based on least error criterion, one structure, shown in table 1, is selected for training of the input-output data. The learning rate is varied in the range of 0.001-0.100 during the training of the input-output data. The network optimization process (training and testing) is conducted for 2000,000 cycles for which stabilization of the error is obtained. Neuron numbers in the hidden layer is varied and in the optimized structure of the network, this number is 6. The number of cycles selected during training is high enough so that the ANN models could be rigorously trained.

Fig.1 presents the optimized three layer network.

Hidden layer (H) Output layer (O) Input layer (I)

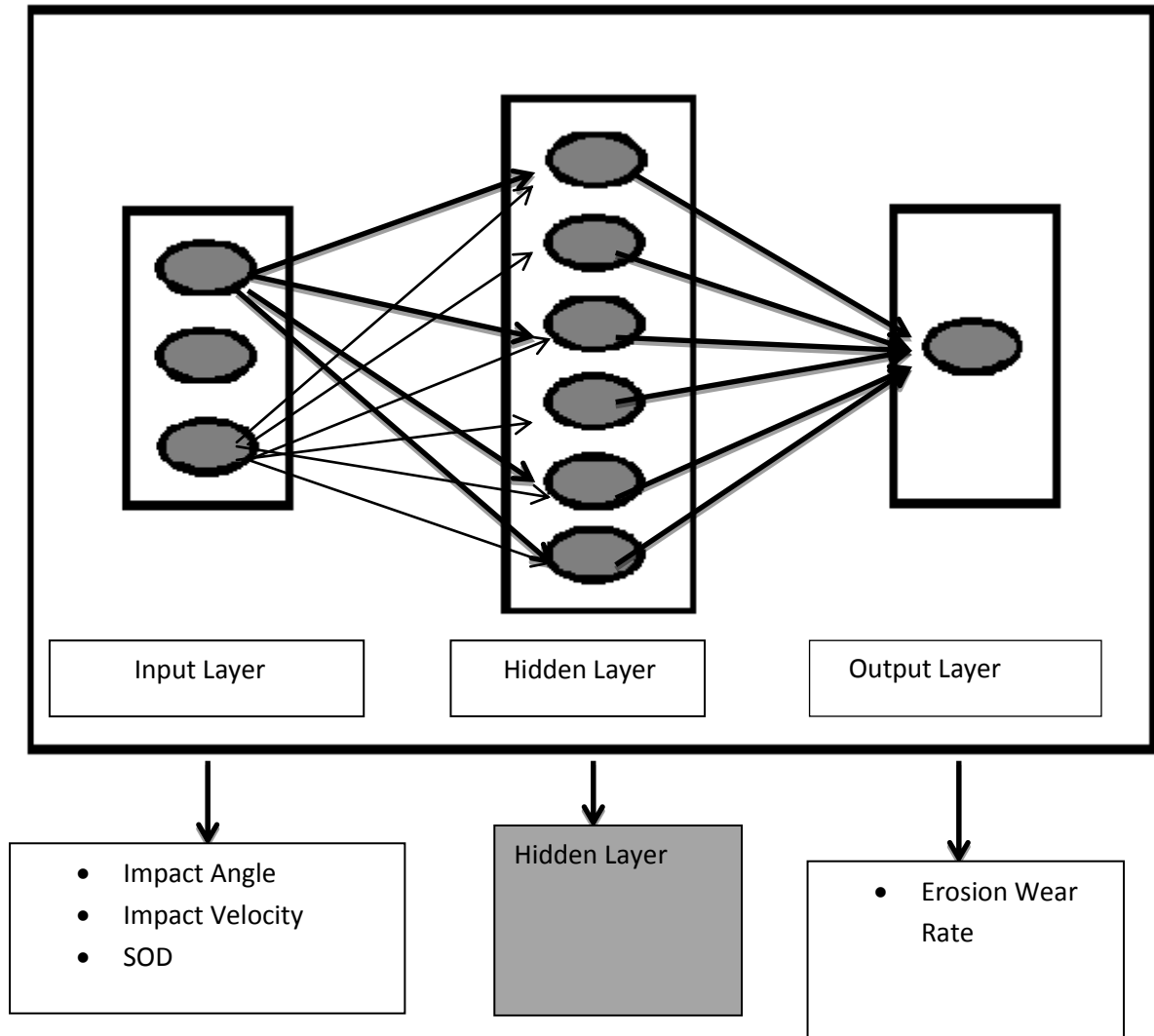


Fig 2.2. The three layer neural network

Chapter 3

EXPERIMENTAL DETAILS

- Introduction
- Sample preparation
 - Erosion wear
- Hardness Measurement
- Roughness Measurement

3.1 Introduction

This chapter deals with the details of the experimental procedures followed in this study. The samples have been first cut into the required dimensions, and then prepared for the further experiments. The specimens have been subjected to a series of tests, e.g., microstructural characterization of the surfaces and cross sections, micro-hardness measurement, X - ray diffraction studies, solid particle erosion wear test etc. The details of each test are described below:

3.2 Sample Preparation

The Al-3Mg-10SiC composite has been fabricated by stir casting technique.[35] A modified stir casting technique for preparation of the Al-Mg alloy is designed using low cost scrap Mg, using a plunger for making the alloy addition. A mild steel cylinder container is coated with aluminium and used to hold the aluminium melt. A hollow spindle which has its stirrer blades attached to motor and V-belt arrangement for better stirring. The plunger rod is attached to perforated capsule which holds the magnesium. Aluminium blocks are melted in the crucible at temperature of 800°C and stirred at 500 rpm. Magnesium turnings are added one after other through the hollow spindle. The magnesium is released after the aluminum foil coating melts and the Mg dissolves in 15 secs. Then the reinforcement SiC particles are added in the similar manner. The melt is poured into moulds and cooled. Then samples of the required dimensions are cut for the erosion wear and other tests.

3.3 Erosion Wear:

In the present work, an erosion apparatus of the 'sand blast' type is used (Fig.3.1) where particles under desired pressure are impinged onto a stationary target. Erosion wear can be conducted over a wide range of particle sizes, velocities, particles fluxes and incidence angles, in order to generate quantitative data on materials and to study the mechanisms of damage. The test is conducted as per ASTM G76 standards.

Samples of size 30mmX 25mmX 3mm were cut and polished with emery paper of grades 1/0, 2/0, 3/0 and 4/0 and were utilized for erosion wear.



Fig 3.1 Erosion wear test setup

3.3.1 Design of Experiment:

Statistical methods have commonly been used for analysis, prediction and/or optimization of a number of engineering processes. The present work addresses to this aspect by adopting a

systematic statistical approach called Taguchi method to optimize the process parameters and save time. The erosion wear tests on the composites are carried out under different operating conditions considering five parameters, viz., impact velocity, standoff distance and impingement angle each at four levels as listed in Table I in accordance with Taguchi's L16 (4^3) orthogonal array. The impacts of these three parameters are studied using this L16 array and the tests are conducted as per this experimental design. The experimental observations are further transformed into signal-to-noise (S/N) ratios. The S/N ratio for minimum wear rate can be expressed as "smaller is better" characteristic, calculated as logarithmic transformation of loss function as shown below.-

$$\frac{S}{N} = -10 \log_{10} \frac{1}{n} (\sum y^2)$$

Where y is the observed data and n is the number of observations

3.3.2 Test Apparatus

Fig.3.2 shows the schematic figure of the erosion test apparatus. The erosion wear testing rig consists of an air compressor, an air drying unit, a magnetic particle feeder, an air-particle mixing and accelerating chamber. A compressor, of maximum compressing capacity of 12 bar is used to compress the air. The compressed air is now let into the erosion wear testing rig where it gets mixed with the particles. The erodent particles are fed at a constant rate from a conveyor belt type feeder present in the mixing chamber and then the erodent particles are accelerated by through a converging nozzle of 4 mm diameter. These accelerated particles impinge the specimen, which can be held at various angles with respect to the impacting particles using an adjustable sample holder. The distance between the particle feeding hopper and belt is monitored

to drive the particles to the mixing chamber that controls the feed rate of the particles. Pressure of the compressed air can be changed to vary the impact velocity of the erodent particles. The velocity of the eroding particles is determined using a double disc method. In the present study, dry silica sand has been used as an erodent. The conditions under which erosion tests were carried out are given in Table 2.

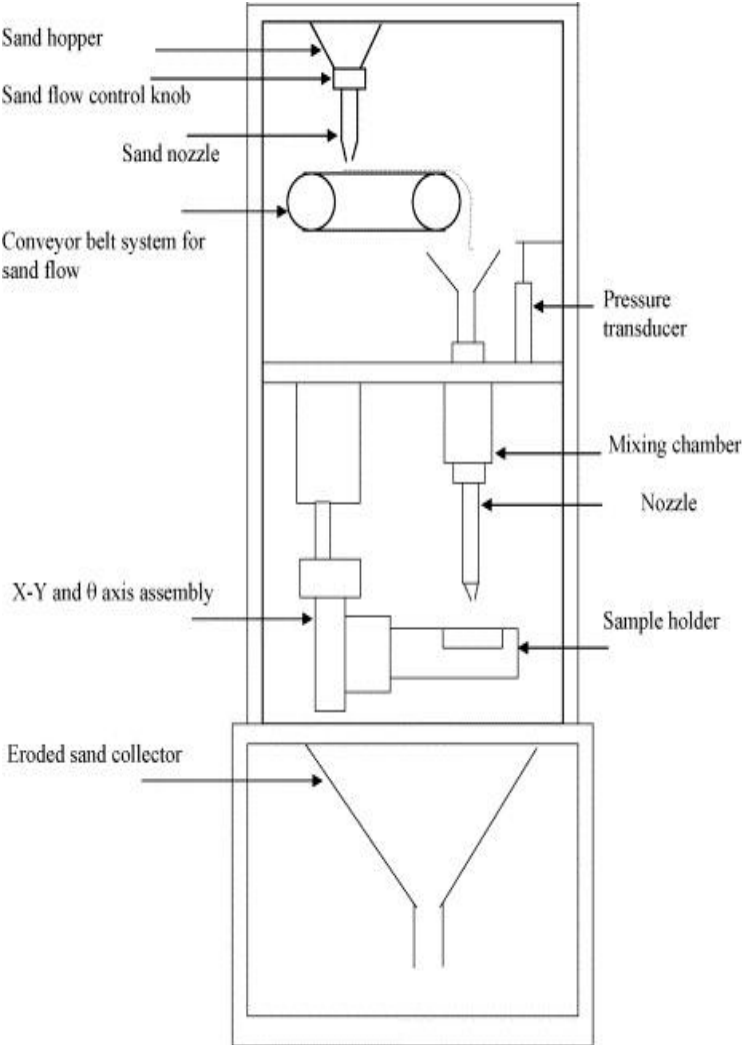


Fig 3. 2. Schematic diagram of erosion test rig

Eroderent	Silica sand
Eroderent size (μm)	150–250
Impingement angle α ($^\circ$)	30, 45, 60, 90
Impact velocity (m s^{-1})	15, 45, 60, 75
Eroderent feed rate (g/min)	12.5
Test temperature	RT
Nozzle to sample distance (mm)	10, 20, 30, 40
Nozzle diameter (mm)	4

Table 2. Erosion test parameters

3.3.3 Experimental Procedure:

1. A standard test procedure was employed for each erosion test.
2. The samples were cleaned in acetone, dried and weighed using electronic balance to an accuracy of 10^{-5}
3. The sample was eroded at a given setup for 10 minutes where it was weighed in every 2 minutes of it and the weight loss was determined. The ratio of this weight loss to the weight of the eroding particles causing the loss (testing time particle feed rate) is then computed as the dimensionless incremental erosion rate value in mg/kg.

$$\text{Wear rate} = \frac{\text{Loss in weight of sample due to erosion}}{\text{Total weight of eroderent}}$$

3.4 Hardness Measurement:

The samples were polished with different sizes of emery papers and finally cloth polished with Alumina (1 μ m). The Vickers's hardness of the polished samples was measured by indentation tests, with a square base diamond indenter under the application of 5N load with a dwell time of 10sec. The diagonals of the indent formed on the surface of the pellet were measured and the hardness was calculated with the following relation:

$$HV = 1.854 \frac{P}{d^2}$$

Where HV is the Vicker's Hardness

P is the load applied

d =(d1+d2)/2 is the average of the diagonals of the indentation on the surface.

3.5 Roughness Measurement:

The surface roughness of the sample is measured at time intervals of 2 minutes during the course of erosion. The roughness is measured by Veeco Dektak 150 profilometer.

Chapter4

RESULTS AND DISCUSSIONS

- Taguchi Analysis
- ANN Prediction of Erosion Wear Rate
 - Optical Microscopy
 - Phase Analysis
 - Hardness
 - Tensile Properties
 - Erosion Wear Test
 - Scanning Electron Microscopy
- Variation of Surface Roughness with Erosion Time

4.1 Taguchi Analysis

The aim of the present study is to minimize the erosion of Al-Mg-10%SiC by optimizing the tribo testing parameters with the help of Taguchi method. The influence of tribological testing parameters like angle of impingement, velocity of impingement and stand-off distance together with their interactions on the erosion behavior of Al-Mg-10% SiC is studied.

Table 3. Response Table for Means

Level	Angle	SOD	Velocity
1	174.79	129.92	49.32
2	108.53	114.57	99.89
3	97.60	116.22	133.29
4	105.63	125.84	204.04
Delta	77.19	15.35	154.72
Rank	2	3	1

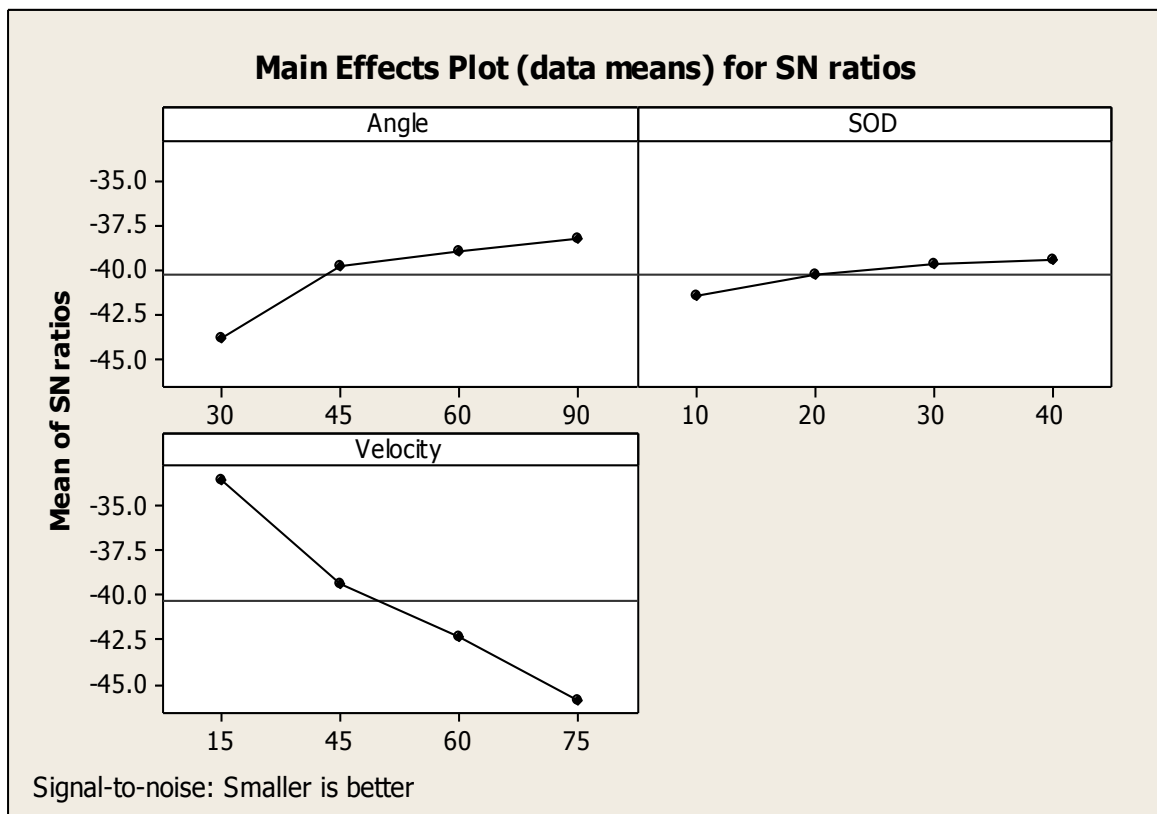


Fig 4.1 Relative Effect of process parameters on erosion wear.

Analysis of Signal-to-Noise Ratio

The desirable factor levels are calculated by simple average of the results. This traditional method is not able to capture the variability of the results within the trial condition. Thus the S/N ratio analysis is done in this study with the friction coefficient as the performance index. The S/N ratio for friction coefficient is calculated using LB criterion and the same is given by

$$\frac{S}{N} = -10 \log_{10} \left(\frac{1}{n} \sum y^2 \right)$$

Where y is the observed data and n is the number of observations. Figure 1 shows the S/N ratio for angle of impingement, velocity of impingement and stand-off distance (SOD). The orthogonal experimental design enables it to separate out the effect of each tribological parameter at different levels. . The mean S/N ratio for each level of the other factors is computed and summarized for each level of factors of angle, SOD and velocity. The response table shows the average of the selected characteristic for each level of the factors. The response table includes ranks based on Delta statistics, which compare the relative magnitude of effects. The Delta statistic is the highest average for each factor minus the lowest average for the same. Ranks are assigned based on Delta values; rank 1 is assigned to the highest Delta value, rank 2 to the second highest Delta value, and so on. The significance of each parameter is determined from the inclination of the main effects plot. A parameter for which the line has the highest inclination will have the most significant effect. It is very much clear from the main effects plot that parameter “velocity” is the most significant parameter while parameter “angle” also has some significant effect. Thus from the present analysis it is clear that the angle of impingement is the most influencing parameter for erosion wear of the composite. Thus minimum erosion occurs at 90o angle, SOD at 40mm and velocity of impingement at 15m/s.

4.2 ANN Prediction Of Erosion Wear Rate

The prediction neural network is tested with three data sets from the original process data. Each data set contained inputs such as impact angle ,impact velocity, stand-off distance and an output value i.e. erosion wear rate is returned by the network. As further evidence of the effectiveness of the model, an arbitrary set of inputs is used in the prediction network. Results are compared to experimental sets that may or may not be considered in the training or in the test procedures. From the table, it is evident that the predicted results show a good agreement with the experimental sets. The optimized ANN structure further permits to study the effect of each of the control input parameters.

Impact Angle (degree)	SOD (mm)	Impact Velocity (m/s)	Erosion Rate (mg/Kg)	ANN Predicted
30	10	15	71.428	77.756
30	20	45	166.667	158.692
30	30	60	180.476	188.192
30	40	75	280.587	273.104
45	10	45	95.238	99.235
45	20	15	47.619	51.513
45	30	75	180.476	165.518
45	40	60	110.793	119.883
60	10	60	130.793	134.326
60	20	75	132.875	139.555
60	30	15	46.492	44.627
60	40	45	80.238	77.364
90	10	75	162.222	174.654
90	20	60	101.111	110.856
90	30	45	57.428	60.677
90	40	15	31.746	34.346

Table 4. Experimental and ANN predicted values which are well in accordance

4.3 Optical Microscopy

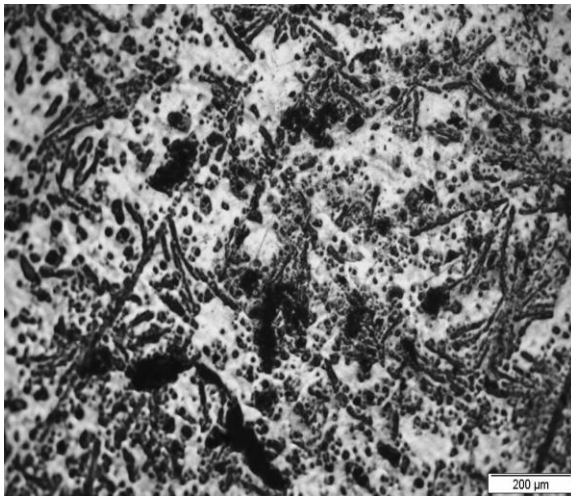


Fig 4.3a

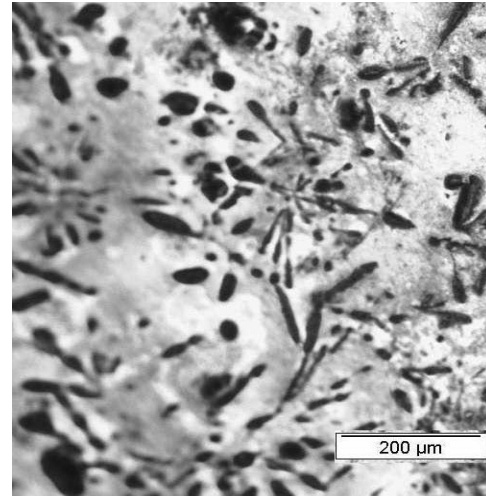


Fig 4.3b

Fig 4.3 Optical microstructures of Al-3Mg-10SiC cast metal matrix composite.

The dark phases, in the above microstructures, are the Silicon carbide particles which are almost homogeneously distributed in the Aluminium-3wt%Magnesium alloy matrix. At some places the SiC particles appear to be in the form of short fibres. This is because of the fact that, the diffusion coefficient of Aluminium-Aluminium and Aluminium-Magnesium is higher than the diffusion coefficient of SiC. Thus the SiC forms clusters by the time the Aluminium-Magnesium matrix gets solidified, exhibiting an elongated type appearance.

4.4 Phase Analysis

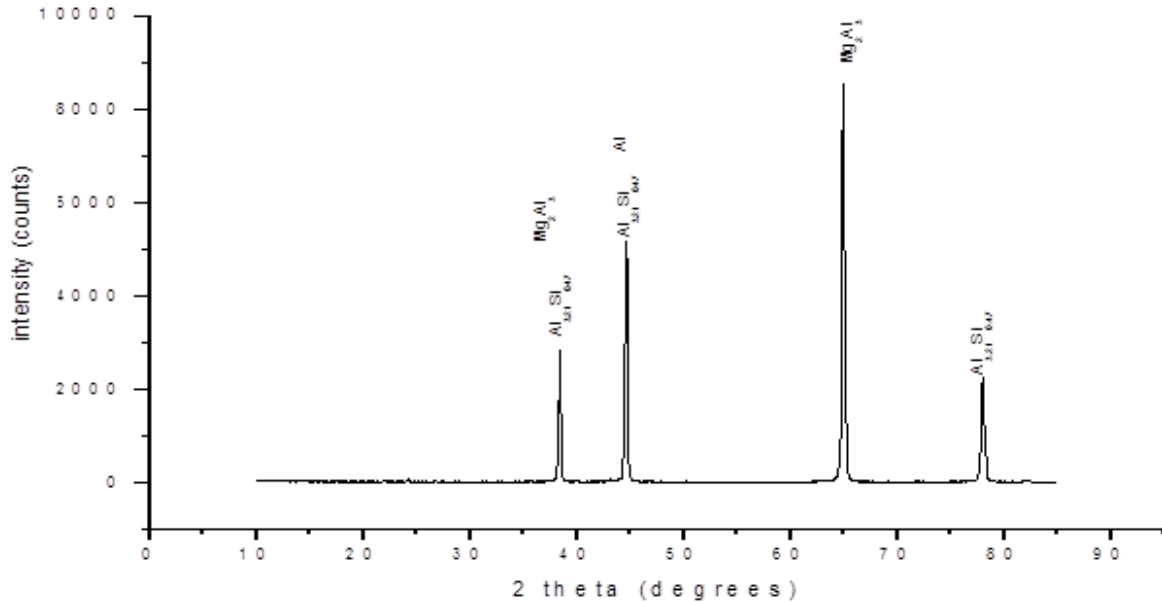


Fig 4.4 XRD plot of the Al-3wt%Mg-10wt%SiC composite

The phase analysis of the sample is done by X-Ray Diffraction. The XRD plot of the uneroded sample shows the presence of different phases. Phases are formed due to the interaction of Aluminium and Magnesium and the SiC particles. Mg₂Al₃ or beta phases in the magnesium aluminium system (also called complex metallic alloy) is found. Another phase Al_{3.21}Si_{0.47} is detected in the composite. This phase may be formed due to the interaction of Aluminium and the SiC particles with the processing route followed.

4.5 Hardness

The hardness of the sample was measured in a Vickers Hardness testing machine with a load of 5 N and a dwell time of 10sec. The Vickers Hardness of the Al-3Mg-10SiC MMC is found to be 124.5HV, (average of 10 measurements). The hardness is found to be higher than that of Aluminium. This may be attributed to the presence of the hard and brittle SiC particles

in the Aluminium alloy matrix. The hardness of the material affects its erosion wear behaviour.

4.6 Tensile Properties

The tensile test of the Aluminium-3wt%Magnesium-10wt%SiC was carried out to determine the tensile strength and material properties. The results are given in table 5:

Ultimate Tensile Strength	43.18 MPa
Yield Stress	31.62 MPa
Young's Modulus	7330 MPa
% Strain at Break	2.003 %

Table 5. Tensile properties of the sample

4.7 Erosion Wear Test

In solid particle erosion wear test, solid erodent particles i.e. dry silica sand strike or impinge on the surface of the material and cause material losses. The solid particles strike the surface at a certain velocity and thus possess momentum and kinetic energy, which they impart to the surface during their impact and result in erosion wear. The particles are impinged at different angles from different standoff distances and at different velocities to study the effect of the process parameters on the erosion wear rate. As the erodent particles strike the surface of the material, different mechanisms of wear come into play depending upon the material characteristics and the process parameters. Experiments are conducted as per the Taguchi Experimental design and the results are extrapolated using Artificial Neural Networking (ANN Analysis).

4.7.1 Variation of Cumulative Mass Loss with Time

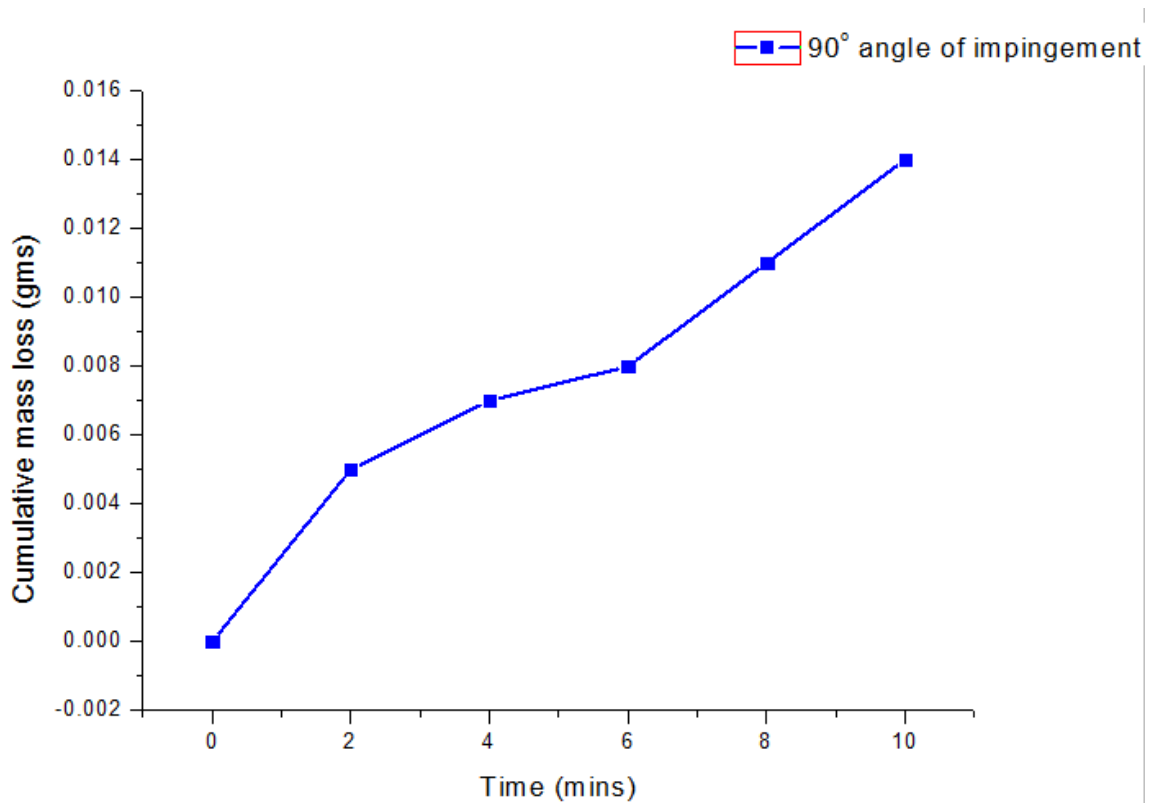


Fig 4.7.1a: Variation of Cumulative Mass loss with time at 90° angle of impact, with a standoff distance of 20mm and impingement velocity of 60 m/s

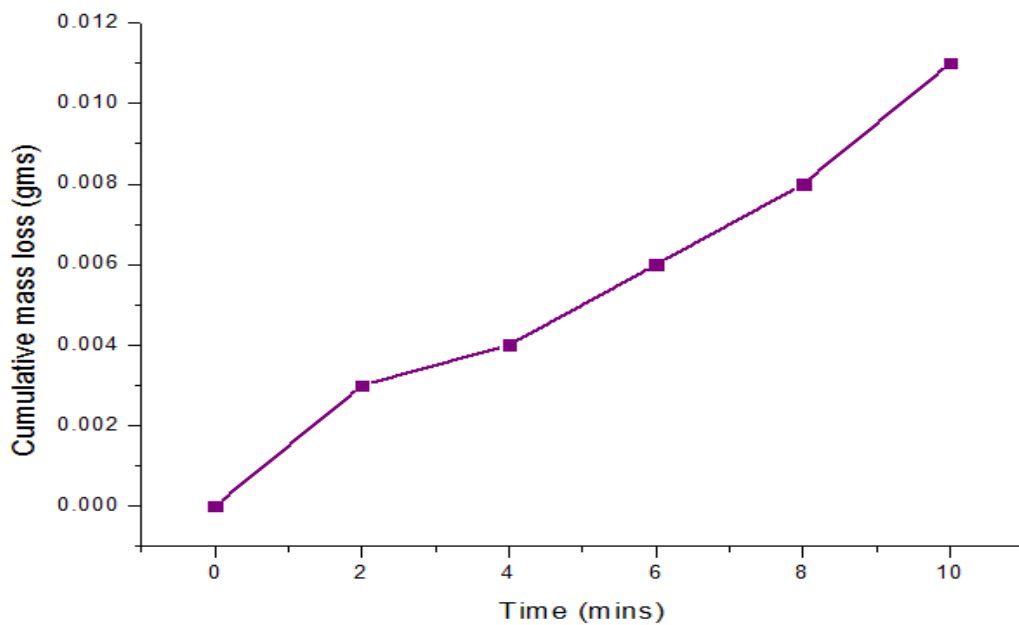


Fig 4.7.1b: Variation of Cumulative Mass loss with time at 45° angle of impact, with a standoff distance of 10mm and impingement velocity of 45 m/s

The Cumulative mass loss versus erosion time, for the sample eroded at 90° are shown in fig 4.7.1a. From the figure it is evident that, there is a sharp increase in the mass loss at the initial stage of erosion i.e. upto 2 mins time. Then the rate of mass loss becomes less (sluggish) up to a certain time length i.e. 6 min erosion time. Then after, the mass loss increases steadily at a constant rate. At initial stage, the erosion is high because the material is soft. But after bombarding for longer time period, the material surface might get hardened for which the material loss rate may be less. Further increase in erosion time i.e. after 6 min, the rate of mass loss increases may be due to development of porous regions on the surface and tearing of grains on the surface.

Figure 4.7.1b shows the cumulative mass loss of the sample versus the time of erosion for sample eroded at 45° . It can be seen that the erosion rate is high in the first two minutes as was the case in erosion at 90° angle. Then the erosion rate becomes sluggish in the next 2mins till 4mins. Then the mass loss again increases steadily after 6 mins till 10mins which may be due to excessive surface tearing during erosion.

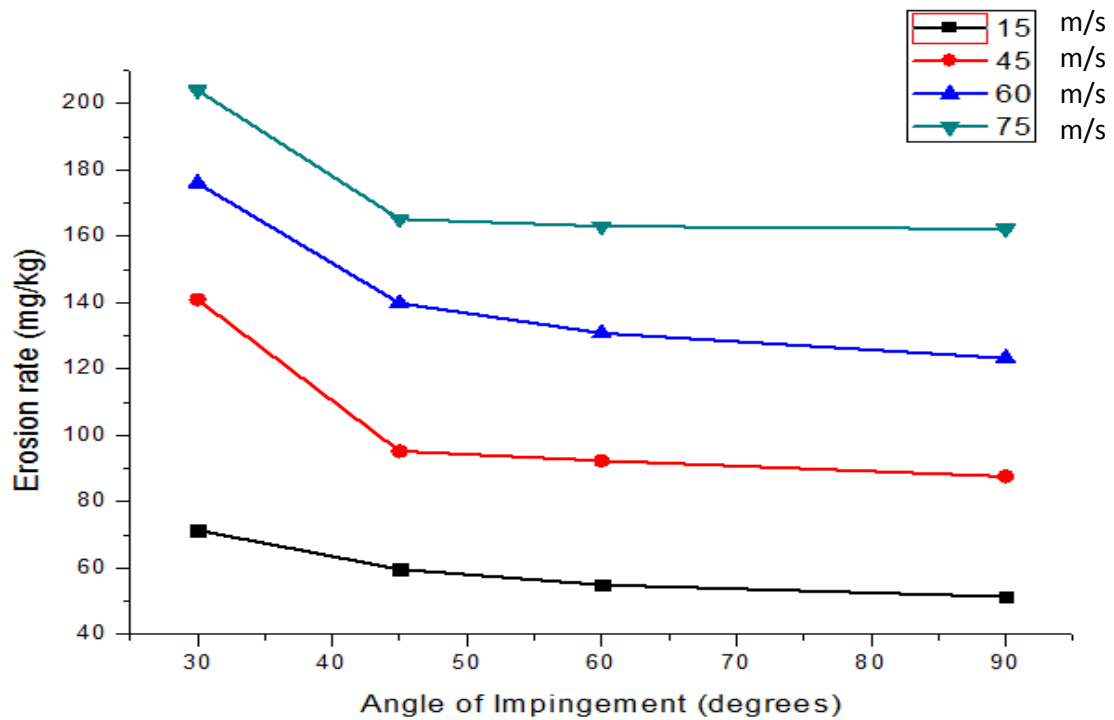


Fig 4.7.2: Variation of erosion rate on impingement angle for different impingement velocities of 15, 45, 60 and 75m/s at standoff distance fixed at 10mm.

Figure 4.7 illustrates the effect of the angle of impingement on the erosion rate of the Al-3Mg-10SiC metal matrix composite when subjected to solid particle (sand) erosion. In the above plot the variation of the erosion rate with impact angle at different pressures is shown. It can be observed from the graph that the erosion rate decreases with the increase in the angle of impact irrespective of the impingement velocities. The erosion wear rate is higher at lower angle of impact and maximum at 30° and decrease till it is lowest at 90° angle. As the maximum erosion occurs at lower angles, it can be said that the erosion occurs by ductile mechanism. Rattan [21] has studied the influence of the angle of impingement on the solid particle erosion rate and suggests that ductile materials show maximum erosion at angle of impingement in the range of 15° to 30° while brittle materials erosion is maximum at 90°.

Ibrahim [37] studied the relationship of the impingement angle on the mechanism of erosion wear and stated that the normal and tangential components of velocity of the erodent particles can be separated and separately control the wear mechanism.

When particles strike, the sample surface at a particular angle, the tangential component of particle velocity results in plastic deformation of the composite [21]. Lower is the impingement angle, greater is the tangential component of the velocity; thus greater is the wear by plastic deformation. As in this particular composite erosion rate is higher at lower angles, thus erosion behaviour is ductile in nature [38]. Bayer[39] has suggested a relationship between the impact angle and the erosion rate in relation to ductile and brittle materials. According to Bayer ductile nature is prevalent at lower angles of 20° to 30° while brittle nature of erosion is dominant in higher angles (90°). Thus the erosion is mainly due to micromachining and ploughing mechanism. At lower impact angles the erodent particles strike the surface and cause maximum erosion by forming grooves as they slide across the ductile surface. It can be seen from the plot that erosion rate is higher at greater velocities. This has also been studied by Alahelisten [40].

4.7.3 Effect of Impingement Velocity

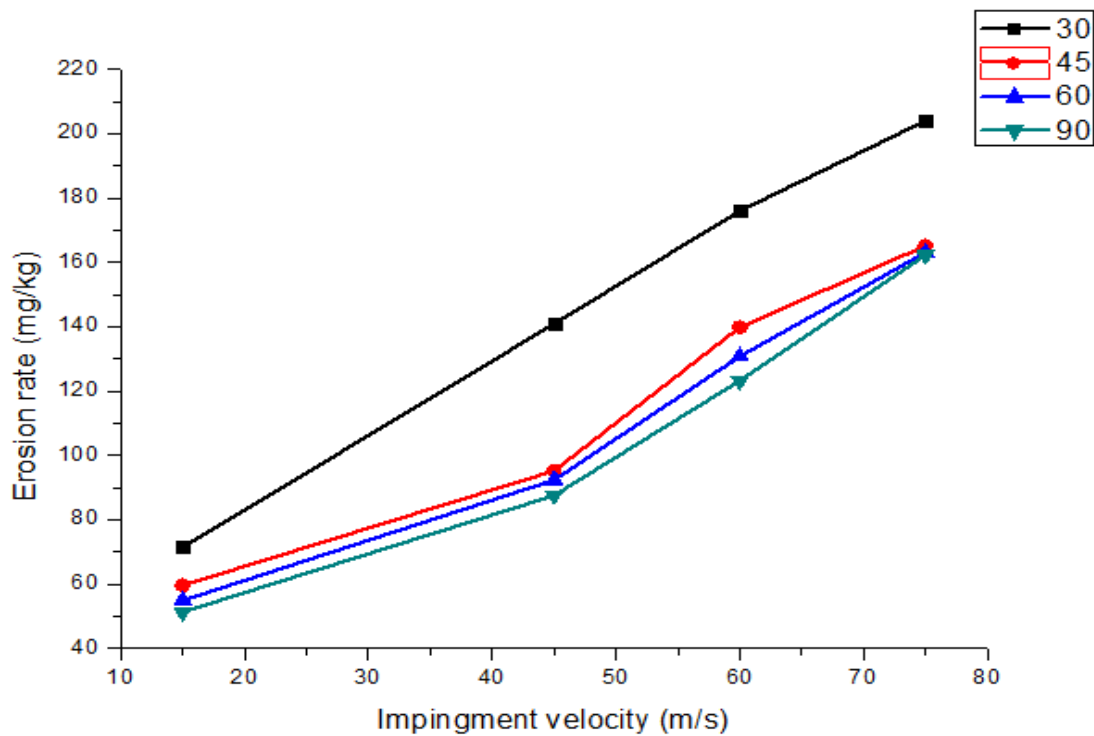


Fig 4.7.3: Variation of erosion rate with impingement velocity for different impingement angles of 30°, 45°, 60° and 90° at standoff distance fixed at 10mm.

The fig 4.7.3 shows the variation of the erosion rate with the change in the velocity of impingement at different angles of impingement. The erosion rate is observed to increase with the increase in the impingement velocity. The higher is the impingement velocity the greater is the momentum and kinetic energy carried by the particles striking the surface, thus greater is the erosion rate. The erosion rate at 30° is seen to be highest as compared to other angles. The erosion rate decreases with increase in the impingement angle. The erosion rates of the angles 45°, 60° and 90° are very close and are nearly similar.

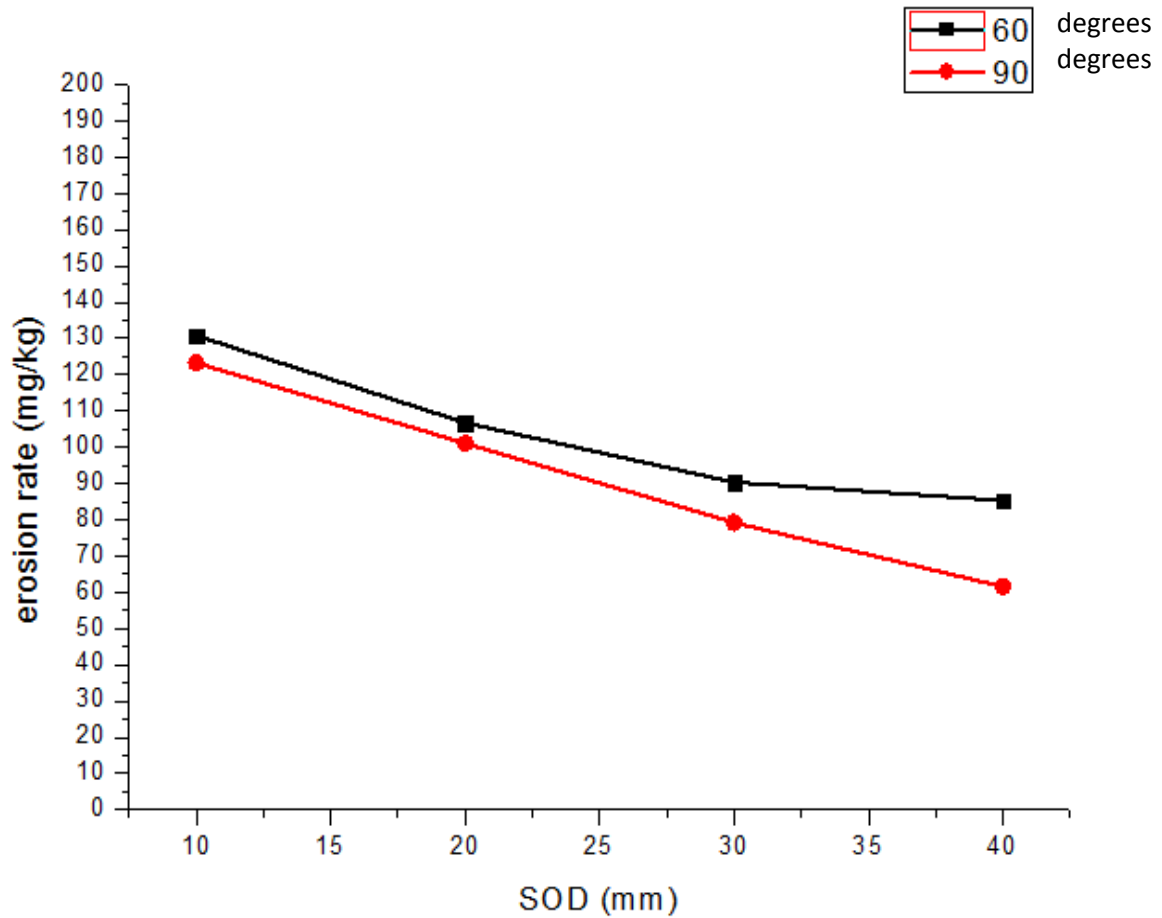


Fig 4.7.4: Variation of erosion rate with Standoff distance(SOD) for different impingement angles 60° and 90° at impingement velocity fixed at 60m/s.

Figure 4.7.4 shows the variation of the erosion rate on the standoff distance at two different impingement angles i.e. at 60° and 90°. It can be seen from the above graph that the erosion rate decreases with the increase in the standoff distance. This can be attributed to the fact that, increasing the standoff distance increases the path travelled by the erodent particles before striking the surface. Thus the particles lose much energy before striking the surface. As the striking velocity is lowered, the erosion rate is also reduced. From the above graph it can be observed that the change in the erosion rate with the SOD is not very significant. The erosion rate at lower angles is greater.

4.8 Scanning Electron Microscopy

The fractured and the eroded surface of the Al-3wt%Mg-10wt%SiC metal matrix composite is observed under the scanning electron microscope. The study of the eroded surface morphology facilitates the investigation of the dominant wear mechanism during solid particle erosion. SEM micrographs of the composite eroded during the course of erosion time are analysed and the wear mechanism is predicted accordingly.

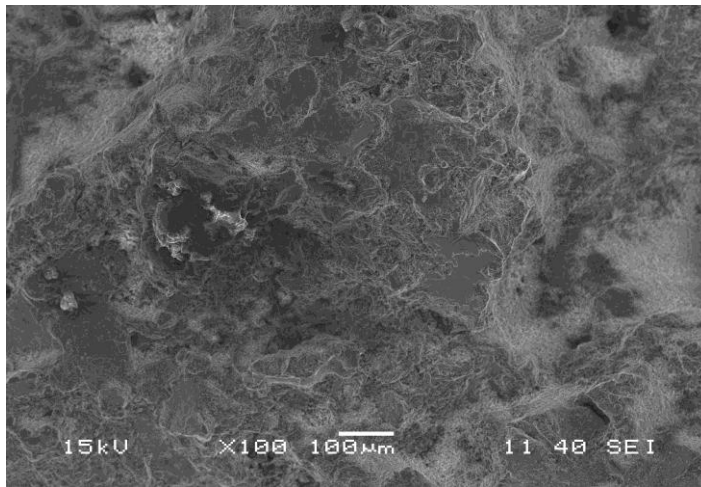


Fig 4.8.1: Fractured surface of Al-3Mg-10SiC composite.

The fractured surface of the sample is dimpled and shows a torn and rugged morphology. There are grooves and pits present and thus it can be concluded that the Al-3Mg-10SiC composites have ductile fracture.

4.8.2 Change in the surface morphology with the erosion time

The Al-3Mg-10SiC composite is subjected to solid particle erosion wear for a time period of 10mins at time intervals of 2mins. The cumulative mass loss of the sample is measured to calculate the erosion wear rate. Scanning electron microscopy is also done after each time interval to study the change in the surface morphology during the course of erosion.

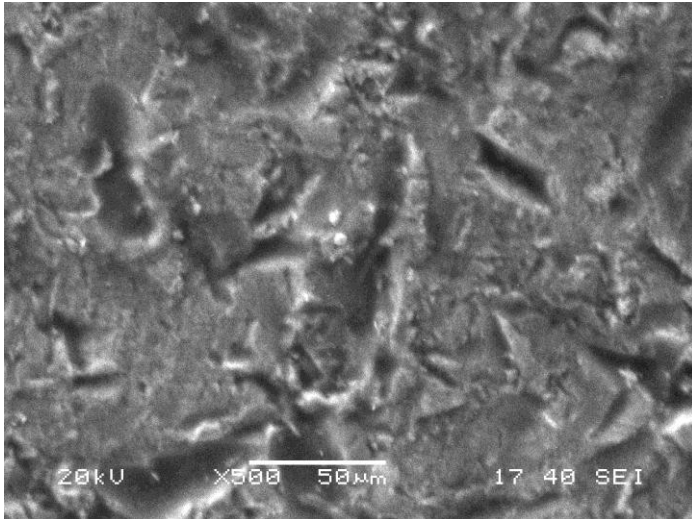


Fig 4.8.2.1a: SEM micrograph of eroded sample at 90° after 2mins. SOD : 20mm, Velocity of impingement: 60 m/s

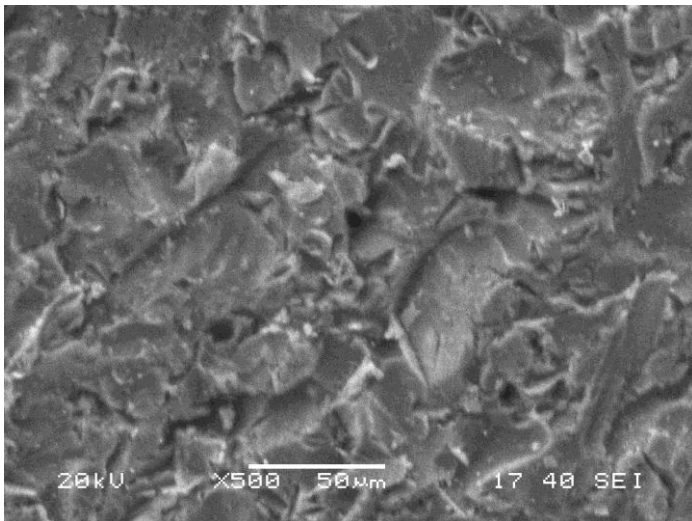


Fig 4.8.2.1b: SEM micrograph of eroded sample at 90° after 4mins. SOD : 20mm, Velocity of impingement: 60 m/s

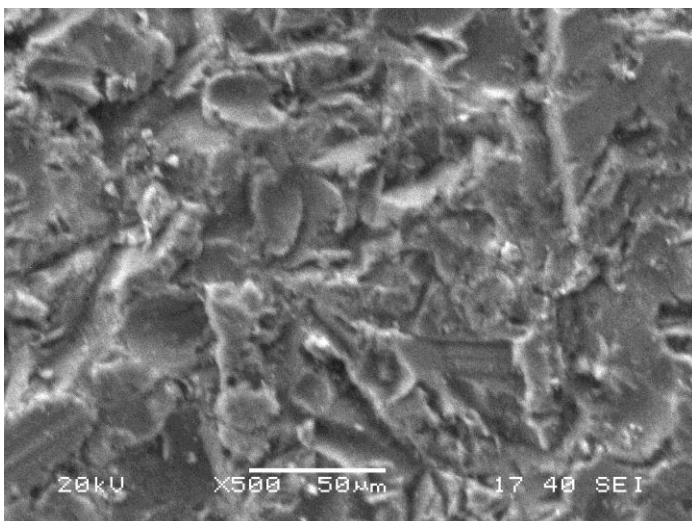


Fig 4.8.2.1c: SEM micrograph of eroded sample at 90° after 6mins. SOD : 20mm, Velocity of impingement: 60 m/s

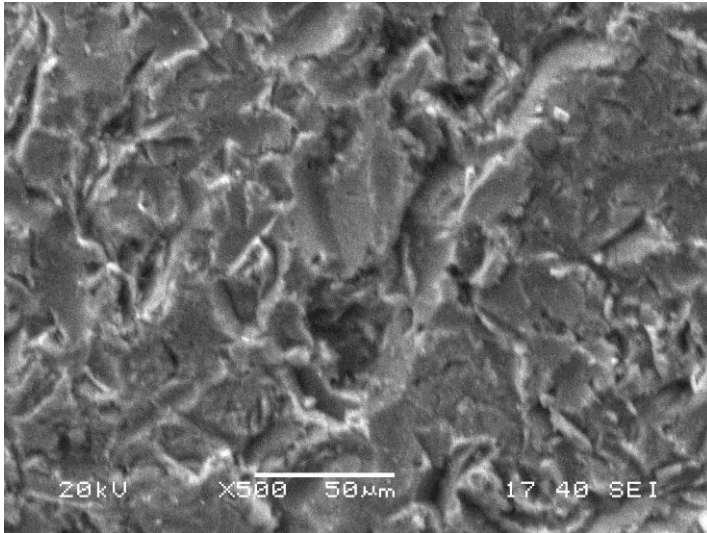


Fig 4.8.2.1d: SEM micrograph of eroded sample at 90° after 8mins. SOD : 20mm, Velocity of impingement: 60 m/s

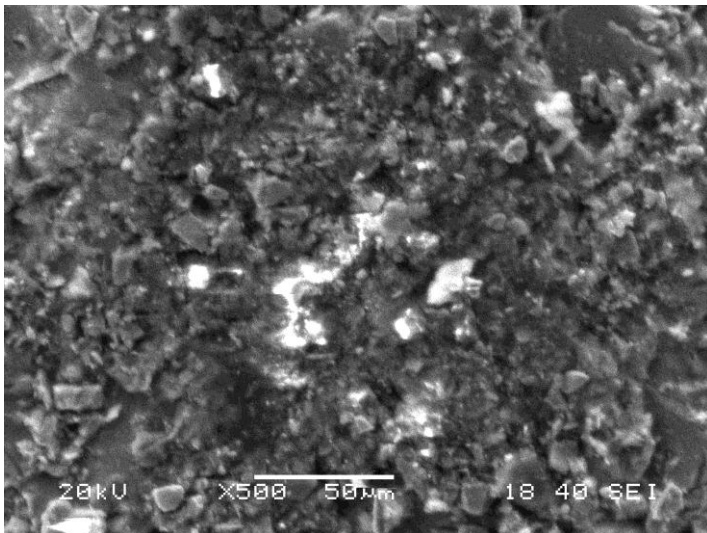


Fig 4.8.2.1e: SEM micrograph of eroded sample at 90° after 10mins. SOD : 20mm, Velocity of impingement: 60 m/s

The surface morphology of the sample eroded at 90° impact angle is shown in the figure 4.8.2.1(a,b,c,d,e). After 2mins of erosion, grooves are observed in the surface but major portion remains flat. The grooves formed are seen to be few but are large (fig 4.8.2.1a).

After 4mins of erosion the amount of cavitations is increased, some cracks are nucleated along the grain boundaries. The formation of these small cavities all over the surface makes the surface more or less smoother and flat (fig 4.8.2.1b).

After 6 mins of erosion time, massive tearing of the surface is seen. Some elongated grooves are also observed (fig 4.8.2.1c). Then as the erosion is further continued for 8mins, massive

amount of material is removed from the surface and some deep grooves are also seen. Cracking of the grains is also noticed. Figure 4.8.2.1e shows the morphology after 10mins of erosion. There is massive cavitation and particles have become smaller due to longer time of impact. No flattened region is observed.

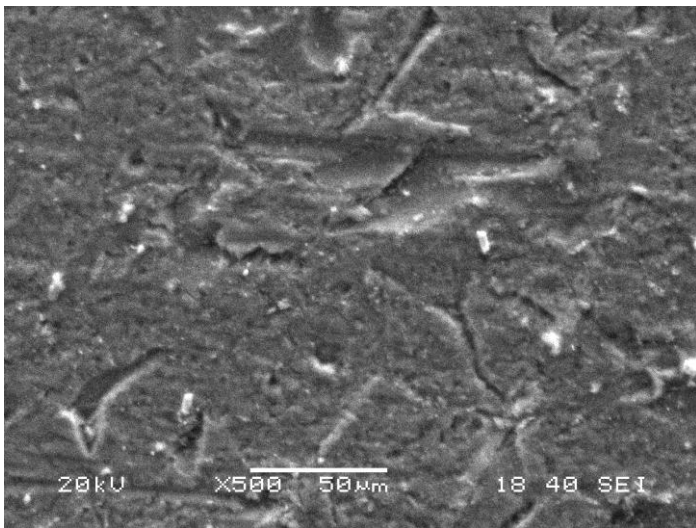


Fig 4.8.2.2a: SEM micrograph of eroded sample at 45° after 10mins.
SOD : 10mm, Velocity of impingement: 45 m/s

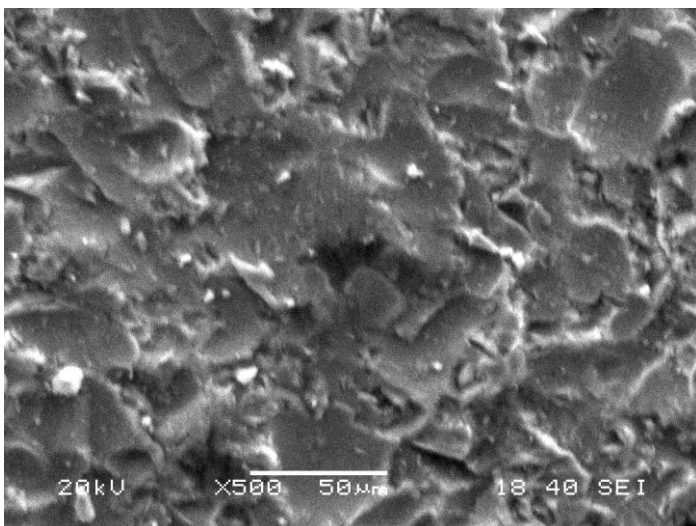


Fig 4.8.2.2b: SEM micrograph of eroded sample at 45° after 10mins.
SOD : 10mm, Velocity of impingement: 45 m/s

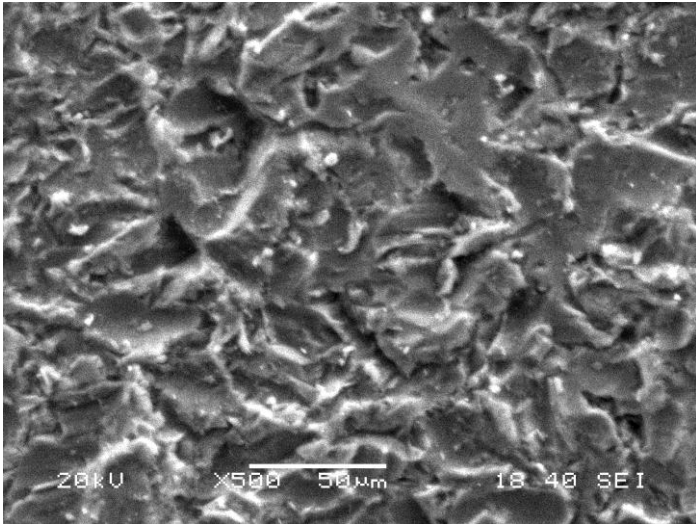


Fig 4.8.2.2c: SEM micrograph of eroded sample at 45° after 10mins.
SOD : 10mm, Velocity of impingement: 45 m/s

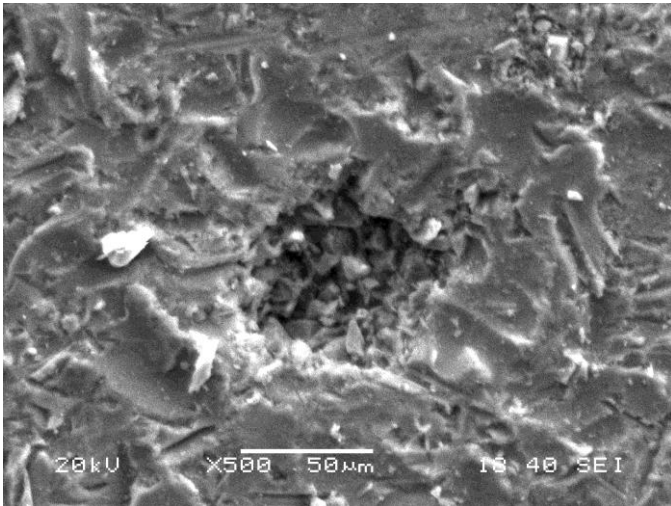


Fig 4.8.2.2d: SEM micrograph of eroded sample at 45° after 10mins.
SOD : 10mm, Velocity of impingement: 45 m/s

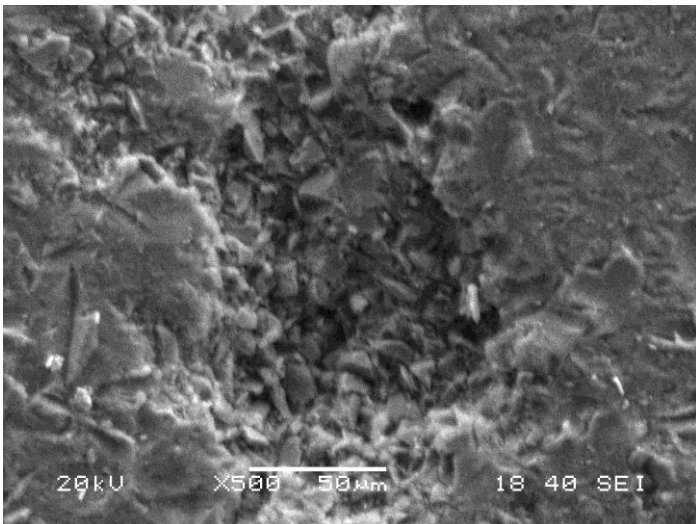


Fig 4.8.2.2e: SEM micrograph of eroded sample at 45° after 10mins.
SOD : 10mm, Velocity of impingement: 45 m/s

The surface morphology of the eroded sample, eroded at 45° impingement angle is shown in figure 4.8.2.2(a,b,c,d,e). At the initial time of erosion i.e. after 2mins, some plastically deformed region is observed and cracks are observed at the grain boundaries (fig 4.8.2.2a). After 4mins the surface morphology is different i.e. tearing of surfaces are observed at many places. Some cavities are also formed at many regions (fig 4.8.2.2b).

After 6mins of erosion, there is massive tearing of the sample surface. The amount of cavities and pits are also increased (fig 4.8.2.2c). Figure fig 4.8.2.2d shows a different type of morphology i.e. formation of deep grooves on the surface is noted. Prominent grooves are formed at particle and grain interface boundaries. After 10 mins of erosion time, the surface morphology is shown in figure fig 4.8.2.2e. Deep elongated grooves are observed on the surface. Some pits are also observed at the sides of the grooves.

4.9 Variation of Surface Roughness with Erosion Time

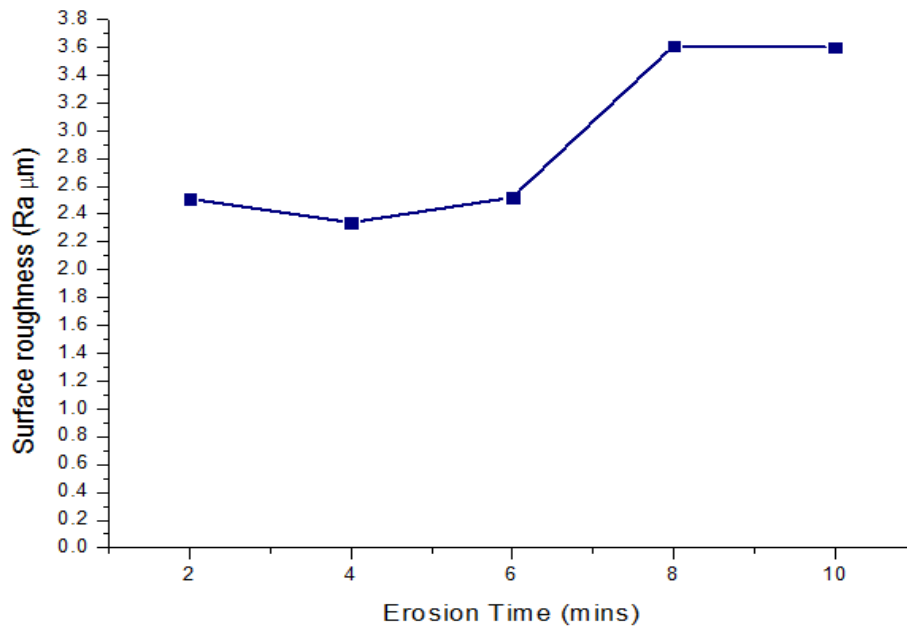


Fig 4.9.1: Variation of the surface roughness of the Al-3Mg-10SiC composite during the erosion time of 10mins. Angle of impact: 90° , SOD : 20mm, Velocity of impingement: 60 m/s

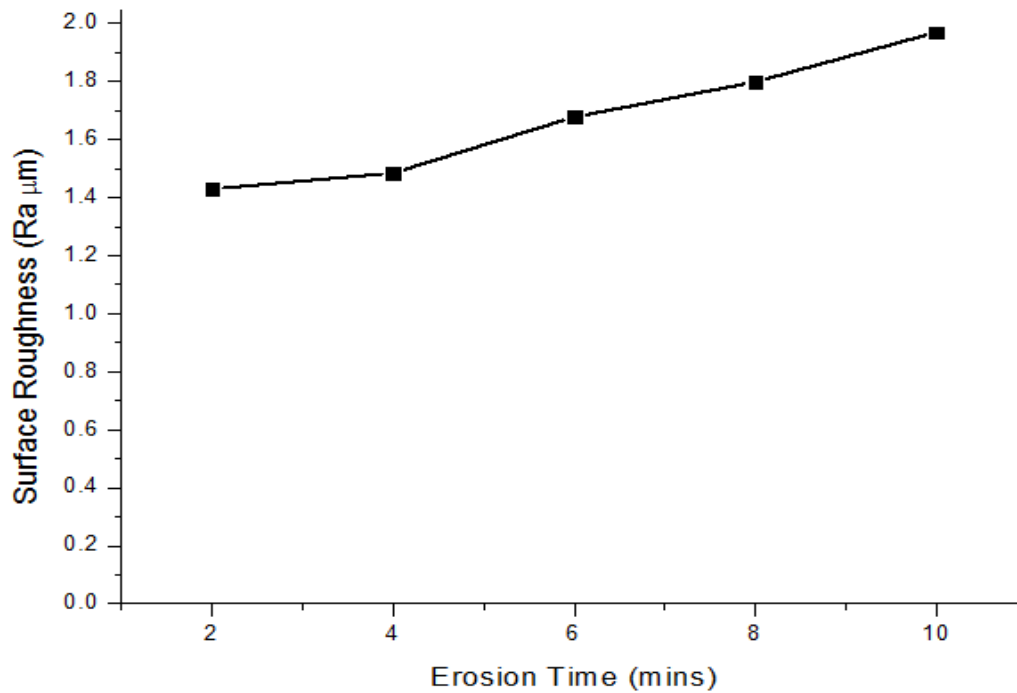


Fig 4.9.2: Variation of the surface roughness of the Al-3Mg-10SiC composite during the erosion time of 10mins. Angle of impact: 45° , SOD : 10mm, Velocity of impingement: 45 m/s

The figure 4.9.1 shows the variation of the surface roughness of the sample with time during the course of erosion wear testing. From the graph it can be seen that the roughness is increased rapidly during the initial time period i.e. in the first 2mins. This also complies to the result of the SEM micrograph and the high cumulative mass loss as seen earlier. This may be because of the material is soft and there is development of many loose protuberances on the surface which are removed first. It can be seen from the graph that, the roughness decreases after 2mins and remains nearly low and steady till 6mins. This may be attributed to the fact that the composite surface gets plastically deformed and thus gets hardened. This results in reduced erosion rate as can be seen in previously. After 6 mins the roughness again increases and maintains a steady level. This results in the steady increase in the cumulative mass loss in the composite after 6mins.

Figure 4.9.2 shows the variation of the surface roughness of the Al-3Mg-10SiC composite with erosion time. It can be seen that the surface roughness increases through the period of erosion wear testing. The roughness is seen to increase rapidly after the first 2mins of erosion wear. Then the roughness is decreased in the next 2mins. This may be due to the hardening of the surface due to plastic deformation caused by the impact of the impinging particles. The roughness increases slightly after 4mins which may be because of formation of pits and grooves on the surface due to the ploughing action of the erodent and the delamination of the SiC particles. Large grooves are observed at the grain-particle interface boundary which may be the cause for the increase in the roughness.

Chapter 5

CONCLUSIONS

5.1 Conclusion:

It is known that Taguchi method is one accepted tool for minimizing the experimental conditions, which gives the idea of the rating of operating factors. In our study we found that Impact velocity is the main operating factor over angle of impact. Based on the above result, experiments were conducted. From the experimental data, ANN analysis is made to find out the results beyond the experimental conditions.

From the XRD results, it is found that the material has Mg_2Al_3 and $Al_{3.21}Si_{0.47}$, as the phases which will have impact on material property. The hardness of this material is found to be 124HV which is more than the hardness of Al-Mg alloy. This may be due to impregnation of SiC particles. From the erosion wear test it is observed that, the wear rate initially is higher with an intermediate sluggishness, it then takes a steady state, irrespective of angle and SOD.

With increase in angle of impingement, the erosion rate reduces, may be due to surface hardening of the material. It is also observed that the variation of erosion rate with impact velocity is maximum.

SOD has the minimum effect on the erosion rate.

From the SEM micrographs, it can be concluded that there are at least two different mechanisms responsible for tribological behaviour; i.e. plastic deformation and brittle fracture.

Examination of variation in surface roughness of the samples eroded at different time lengths indicate the operation of at least two different mechanisms (Fig 4.9.1 & 4.9.2)

All the above observations imply that the material can be a suitable for some mechanical components used in automobiles applications.

References

REFERENCES

- [1] R. Guè rler, Sliding wear behavior of a silicon carbide particle±reinforced aluminum±magnesium alloy, *JOURNAL OF MATERIALS SCIENCE LETTERS* 18 (1999) 553±554
- [2] Kinga A.Unocic, ”Structure Composition Property Relationships in 5XXX series Aluminium Alloys”Ohio State University 2008
- [3].Kaufman J.Gilbert, Rooy Elwin L.Aluminium alloy casting: Properties, Process and Applications.ASM International, December 2004
- [4]. Miller W.S. , Zhuang L. , Bottema J. , Wittebrood A.J. , Smet P. De , Haszler A. , Vieregge A.. Recent development in aluminium alloys for the automotive industry, *Materials Science and Engineering A280* (2000):pp. 37–49
- [5] Mazzolani Federico.Aluminium alloy structures. London: Chapman & Hall, 1995
- [6] SURAPPA M K. Aluminium matrix composites: Challenges and Opportunities. *Sadhana* Vol. 28, Parts 1 & 2, February/April 2003, pp. 319–334
- [7]- Si-wei Zhang ,Tribology of elastomers, Elsevier, 2004, Pg. 02
- [8] Horst Czichos ,Tribology: a systems approach to the science and technology of friction,lubrication and wear, Elsevier, 2009, Pg: 11
- [9] Williams John Austin, “Engineering Tribology”, New York, Cambridge University Press, 2005, page-165
- [10] Soda N., ‘Wear of some F.F.C metals during unlubricated sliding part-1.Effects of load, velocity and atmospheric pressure on wear’. *Wear*. Volume33, (1975):p. 1-16.
- [11] Burwell J.T. and Strang C.D, ‘Metallic wear’, *Proc. Soc (London)*, 212A May 1953, p. 470-477.
- [12] Burwell J .T. , ‘Survey of possible wear mechanisms.’ *Wear*. Volume1, (1957/58): p.119-141.
- [13] S.M.Walley, J.E. Field, The erosion and deformation of polyethylene by solidparticle impact, *Philosophical Transactions of the Royal Society, London A* 321 (1987) 277–303.
- [14] P.V. Rao, D.H. Buckley, Angular particle impingement studies of thermoplastic materials at normal incidence, *ASLE Transactions* 29 (1986) 283–298.
- [15] D.R. Andrews, An analysis of solid particle erosion mechanisms, *Journal of*

Physics D: Applied Physics 14 (1981) 1979–1991.

[16] K. Friedrich, Erosive wear of polymer surfaces by steel blasting, *Journal of Materials Science* 21 (3) (1986) 3317–3332.

[17] J.C. Arnold, I.M. Hutchings, A model for the erosive wear of rubber at oblique impact angles, *Journal of Physics D: Applied Physics* 25 (1992) A212–A229.

[18] K.J. Gross, Dissertation, Universität at Stuttgart, 1988.

[19] A. Alahelsten, F. Bergman, M. Olsson and S. Hogmark, On the wear of Aluminium-Magnesium metal matrix composites, *Wear*, 165 (1993) 221-226

[20] J.D. Ayers, Wear behavior of carbide-injected titanium and aluminum alloys, *Wear*, Volume 97, Issue 3, 15 September 1984, Pages 249–266

[21] R.Rattan, Jayashree Bijwe, "Influence of impingement angle on solid particle erosion of carbon fabric reinforced polyetherimide composite", *Sci. Technol. Adv. Mater.* 8, 023102, 2002

[22] S. Wilson and A. Ball, Wear resistance of an aluminium metal matrix composite, in P.K. Rohatgi, P.J. Blau, and C.S. Yust (eds.), *Tribology of Composite Materials*, ASM International, Metals Park, OH, 1990, pp. 103-112.

[23] G.S. Peace (1993). *Taguchi Methods*. Addison-Wesley Publishing Company.

[24] J.H. Lochner and J.E. Matar (1990). *Designing for Quality*. ASQC Quality Press.

[25] W. Y. Fowlkes and C.M. Creveling (1995). *Engineering Methods for Robust Product Design*. Addison-Wesley Publishing Company.

[26] S.H. Park (1996). *Robust Design and Analysis for Quality Engineering*. Chapman & Hall.

[27] M.S. Phadke (1989). *Quality Engineering Using Robust Design*. Prentice-Hall.

[28]. Taguchi G., *Introduction to quality engineering*, Asian Productivity Organization (1990)

[29]. Ross P. J., *Taguchi Technique for Quality Engineering* 2nd edn (1996)

[30]. Roy R.K., *A primer on Taguchi method*, New York: Van Nostrand Reinhold (1990)

- [31] Z. Zhang, K. Friedrich, Artificial neural network applied to polymer composites: a review, *Comp. Sci. Technol.*, in press.
- [32] V. Rao and H. Rao , 2000, '*C++ Neural Networks and Fuzzy Systems*' BPB Publications.
- [33] S. Rajasekaran , G. A. Vijayalakshmi Pai --*Neural Networks, Fuzzy Logic And Genetic Algorithms—Synthesis and Applications* -Prentice Hall of India Pvt. Ltd. , New Delhi (2003)
- [34] Alok Satpathy, S.C.Mishra, Rojaleena Das, S.S. Mishra, P.V. Ananthapadmanabham and K.P. Shree Kumar, Prediction of Erosion behaviour of Plasma Sprayed Fly Ash Coating using Neural Network, presented in DAE-BRNS Symposium on Power Beam Applications in materials processing PBAMP2006, BARC, Mumbai
- [35] B. P. Samal, A.K. Misra, S.C. Panigrahi, B. Sarangi, S. Mishra, A Novel Technique for improving the recovery of Mg in preparation of Al – Mg alloy by casting route.
- [36] Amar Patnaik,* , Alok Satapathy, Navin Chand, N.M. Barkoula, Sandhyarani Biswas, Solid particle erosion wear characteristics of fiber and particulate filled polymer composites: A review, *Wear* 268 (2010) 249–263
- [37] A.T Ibrahim, A mechanisms for solid particle erosion in ductile and brittle materials, MS Thesis, Wichita State University, (1990).
- [38] K.V.Pool, C.K.H. Dharan and I. Finnie, "Erosion Wear of Composite Materials", *Sci. Technol. Adv. Mater.* 9, 033002, 2008
- [39] Bayer G. – Mechanical Wear Prediction and Prevention – Marcel Dekkar, Inc., New York: (1994) pp.396
- [40] A. Alahelsten, P. Hollman and S. Hogmark, Solid particle erosion of hot flame deposited diamond coatings on cemented carbide. *Wear*. Volume 117, (1994): p. 159-165